

Project 3: Flow over a Three-Element Airfoil

AE523, Computational Fluid Dynamics, Fall 2016

Tzu-Hsiang Lin ^{*}

1 Introduction

In this project, the first and second-order finite volume method will be applied for solving a compressible, subsonic flow over a three-element, high-lift device airfoil. In the postprocessing, the resulting forces, lift and drag coefficients, Mach and pressure contours and streamlines will be shown.

This report is arranged as follows. The project begins in section 2 with the geometry, parameters setting and numerical methods. In section 3, the results of first-order finite volume scheme with two coarse meshes: 1149 and 2116 elements will be discussed. In section 4, second-order finite scheme will be applied on the previous meshes. In section 5, two more dense meshes, 4124 and 8031 elements, will be used for comparing the difference between first and second-order finite volume method. Some conclusions will be discussed in section 6 and some larger graphs will be shown in the Appendix.

2 Geometry, Parameters and Numerical Methods

The case airfoil with chord length, $c = 0.588$, is shown in Figure 1, which consists of three parts: leading edge slat, main portion, and the trailing edge flap. Convenient units for the free stream flow conditions are: $\rho = 1$, $M_\infty = 0.25$, $\gamma = 1.4$, and the angle of attack is 5 degree. For numerical method, both first and second-order finite volume methods will be implemented to solve the case, and time marching is using local time step for both methods. The solution will be deemed as converged if the L_∞ norm of the residual is less than 10^{-7} . Moreover, for updating the state, Forward Euler will be used for the first-order method, and the TVD RK2 scheme will be used for second-order.

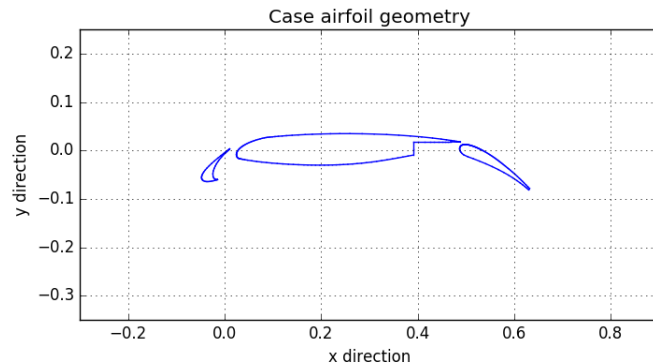


fig. 1: The initial condition of the density distribution of a traffic flow equation.

¹email: tzuhslin@umich.edu

3 First-order Finite Volume Method

3.1 Implement a first-order finite volume method on given meshes

In the zipped files, there are five individual python files, named in *runfv2D.py*, *fv2D.py*, *mesh.py*, *flux.py* and *post.py*. For loading and processing mesh files are coded in *mesh.py*. The first-order volume method is coded in the function named *firstorderfv* in *fv2D.py* and *flux.py*. For lift and drag coefficient calculation are coded in *post.py*.

3.2 Run the codes on two meshes: mesh 0 and mesh 1

Here, mesh 0 and mesh 1 indicates the different mesh elements, 1149 and 2116 elements, respectively. To run the code, a user just need to set up the mesh type and indicates which scheme he or she wants, first-order or second-order, in *runfv2D.py* file. And the corresponding results are listed below.

3.2.1 Plot the residual and C_l convergence with iterations

Figure 2 shows how first-order finite volume scheme converge. Recall the criteria for convergence is when the maximum residual(L_∞ norm) below than 10^{-7} . It is clear to see that, for mesh 1, 2116 elements, it takes more iterations than mesh 0, 1149 elements, takes to converge; however, the oscillation pattern between these two meshes are still quite similar. On the other hand, because the residual convergence will only be plotted every 10 iterations, the graph may not show that the residuals reach 10^{-7} .

Similar trend can also be observed in Figure 3, C_l convergence. In lift coefficient convergence, the oscillation in mesh 0 and mesh 1 are similar before it starts to converge. However, for denser mesh, mesh 1, the C_l is slightly higher than mesh 0. More specific lift and drag coefficient results are discussed in section 3.2.2.

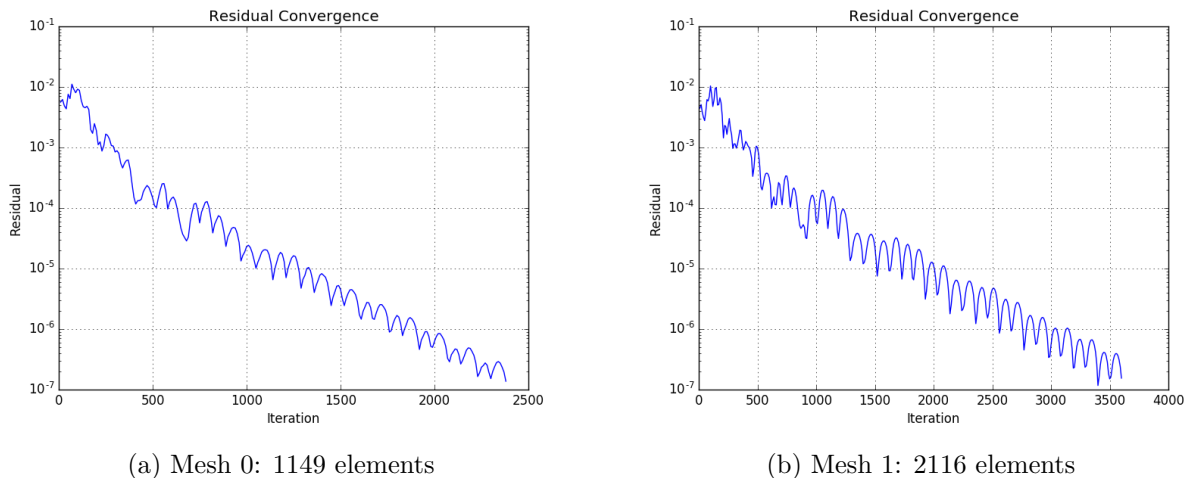


fig. 2: Residual convergence for mesh 0 and mesh 1 with first-order finite volume method implementation.

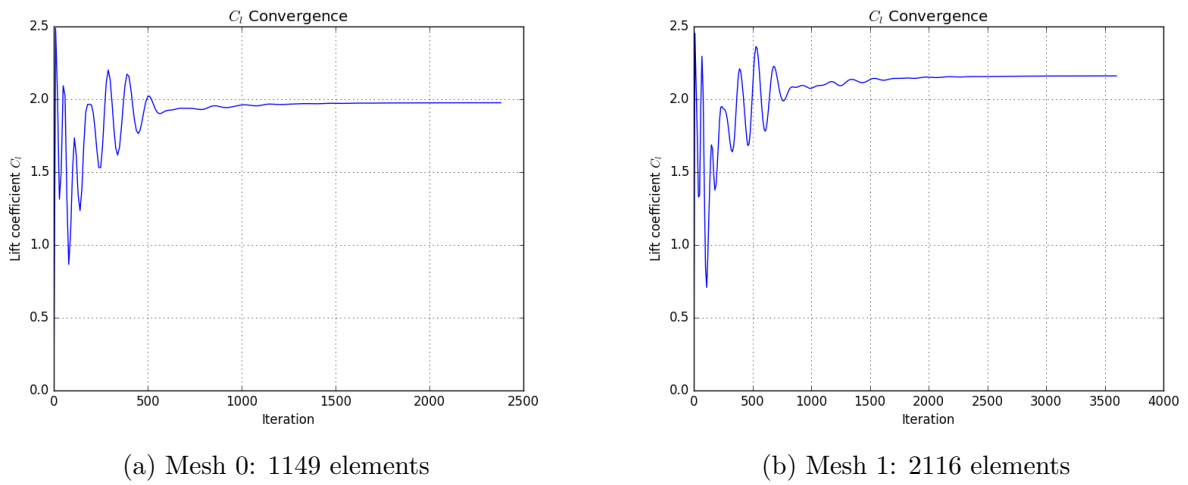


fig. 3: Lift coefficient convergence for mesh 0 and mesh 1 with first-order finite volume method implementation.

3.2.2 The total C_l and C_d values

(a) mesh 0: 1149 elements				(b) mesh 1: 2116 elements				
	total	main	slat		total	main	slat	flap
C_l	1.9761	1.5261	0.0078	0.4422	2.1608	1.6670	0.0273	0.4664
C_d	0.3147	-0.0078	0.0495	0.2730	0.2812	-0.03019	0.0354	0.2761

Table 1: The lift and drag coefficient for mesh 0 and mesh 1 with first-order finite volume method implementation.

In this subsection, the difference of the lift and drag coefficient between two different meshes will be discussed. Since this is an airfoil with slat and flap elements, the lift and drag coefficients contributed from each part are listed in Table 1. Table 1 indicates that the total lift coefficient of mesh 1 is slightly higher than mesh 0(roughly 0.2 difference), and for drag coefficient, mesh 1 has lower value than that of mesh 0, which leads to a more reasonable L over D value. Despite the difference between total values, two meshes show that the main wing dominates the lift coefficient and, surprisingly, has negative value of drag coefficient.

3.2.3 The Mach and pressure contours

The contour of Mach number and pressure can provide us a direct information. From Mach number contour, shown in the Figure 4, both mesh 0 and mesh 1 show that the flow on upper surface has higher velocity than lower surface, which is under my expectation. However, mesh 1 tends to give a more subtle Mach number distribution around the airfoil elements.

For pressure contour, shown in Figure 5, the pressure above the airfoil is less than the bottom of it, which is under expectation too. However, the difference of pressure contour between mesh 0 and mesh 1 is not as clear as that of the Mach number contour shows.

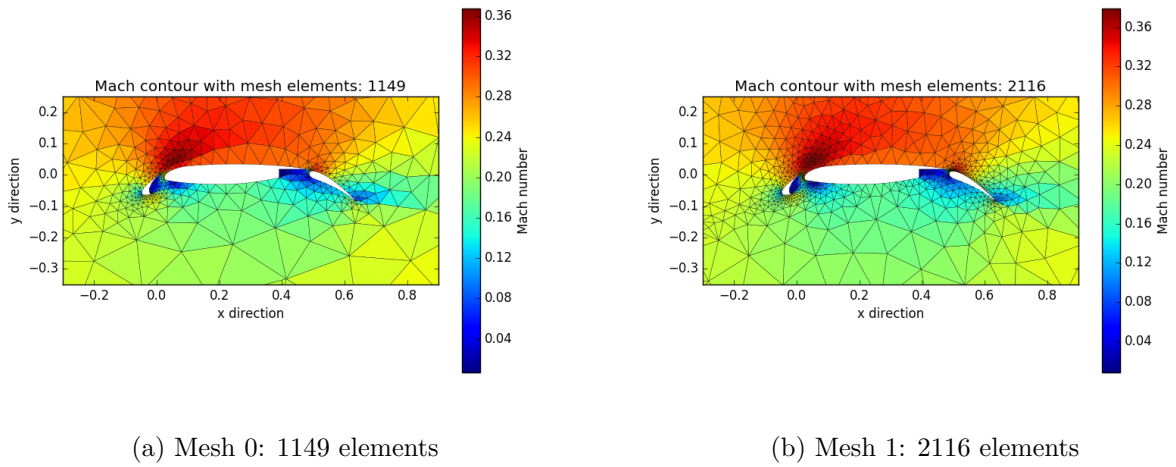


fig. 4: Mach number contour for mesh 0 and mesh 1.

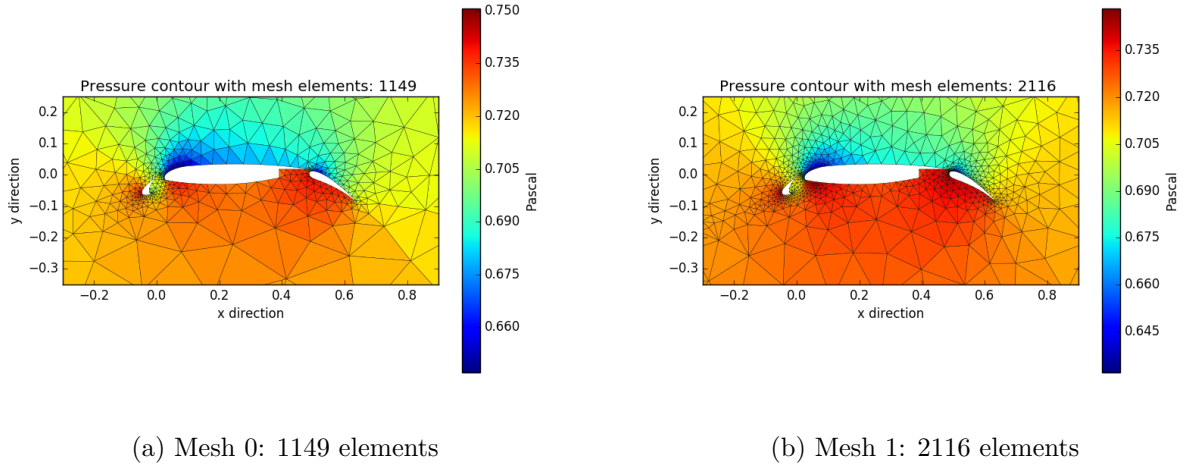


fig. 5: Pressure contour for mesh 0 and mesh 1.

3.2.4 The surface pressure coefficient, C_p , distribution

As we know that the pressure exert on the surface of an airfoil dominates the resulting force, which leads to lift and drag, directly. Plotting out the distribution of the pressure coefficient can make us easily understand the function of each part of an airfoil. Figure 6 indicates that the flap leads to a considerable pressure difference between upper and lower airfoil, which increases the lift on the airfoil but also momentum.

On the other hand, the slat does not contribute as much pressure difference as flap does, however, the main function for slat is try to delay the stall angle of attack but not increase lift.

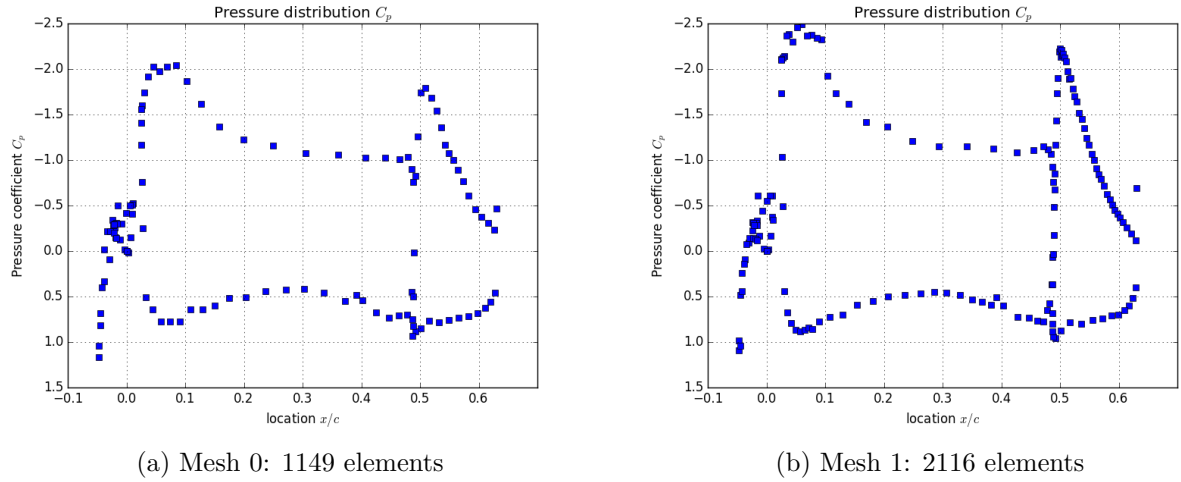


fig. 6: Pressure Coefficient(C_p) contour for mesh 0 and mesh 1.

3.3 Plot the streamlines and calculate the mass flow rate in the slat/main and main/flap gaps.

Figure 7 shows how the air flow over the airfoil, and Table 2 indicates the unit mass flow rate between main/slap and main/flap gaps. Overall, both meshes share a similar streamline pattern and provide the proof that some airflow, indeed, flows through the gaps between airfoil elements, contribute the mass flow rate in Table 2.

(a) mesh 0: 1149 elements		(b) mesh 1: 2116 elements	
gap location	mass flow rate	gap location	mass flow rate
slap/main	0.003441	slap/main	0.004054
flap/main	0.001684	flap/main	0.001870

Table 2: Mass flow rate between the main/slap, main/flap gaps, for mesh 0 and mesh 1.

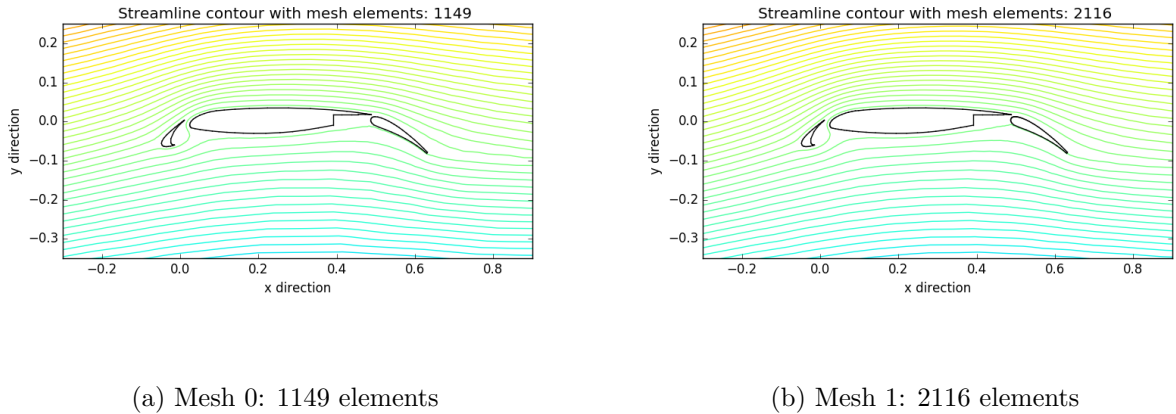


fig. 7: Streamline contour for mesh 0 and mesh 1.

4 Second-order Finite Volume Method

4.1 Implement a first-order finite volume method on given meshes

Other than using first-order finite volume method, a second-order scheme usually provide a higher accurate solution. The corresponding codes are coded in the function named *secondorderfv* in *fv2D.py*. Same as first-order, the results from second-order scheme, such as: lift, drag and pressure coefficients, streamline, Mach number and total pressure contours, will be shown in this section. However, the Mach and pressure contours will be plotted with linear variation.

4.2 Run the codes on two meshes: mesh 0 and mesh 1

Similarly, mesh 0 and mesh 1 will be used as the testing meshes. To implement the second-order scheme, simply set the order equal to 2 in the *runfv2D.py* file.

4.2.1 Plot the residual and C_l convergence with iterations

Figure 8 shows how second-order finite volume scheme converge. Here, the criteria for convergence remains when the maximum residual(L_∞ norm) below than 10^{-7} ; recall that the residual may not reach 10^{-7} on the graph, because they are plotted only every 10 iterations. It is clear to see that, for mesh 1, 2116 elements, it takes about 1000 iterations more than mesh 0, 1149 elements, takes to converge, however, compare to first-order, both meshes require more iterations to converge. For oscillation pattern, although the period between two meshes are quite similar, the magnitudes are quite different.

C_l convergence, in Figure 9, shows that the C_l for mesh 0 and mesh 1 soar to 3.05 and 3.24, respectively. Unlike first order method, the data between two meshes do not have too much difference. More specific lift and drag coefficient results are discussed in section 4.2.2.

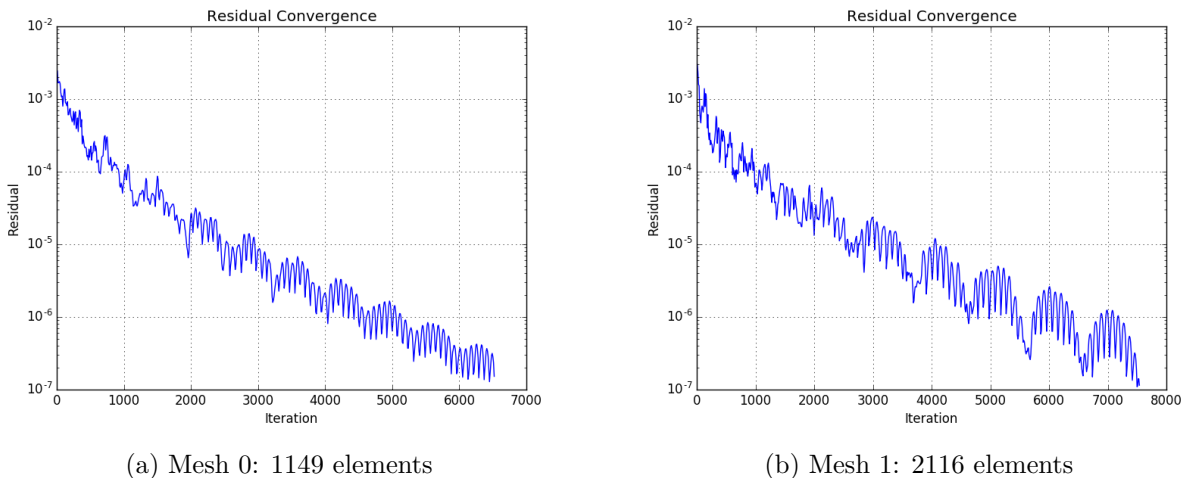


fig. 8: Residual convergence for mesh 0 and mesh 1 with second-order finite volume method implementation.

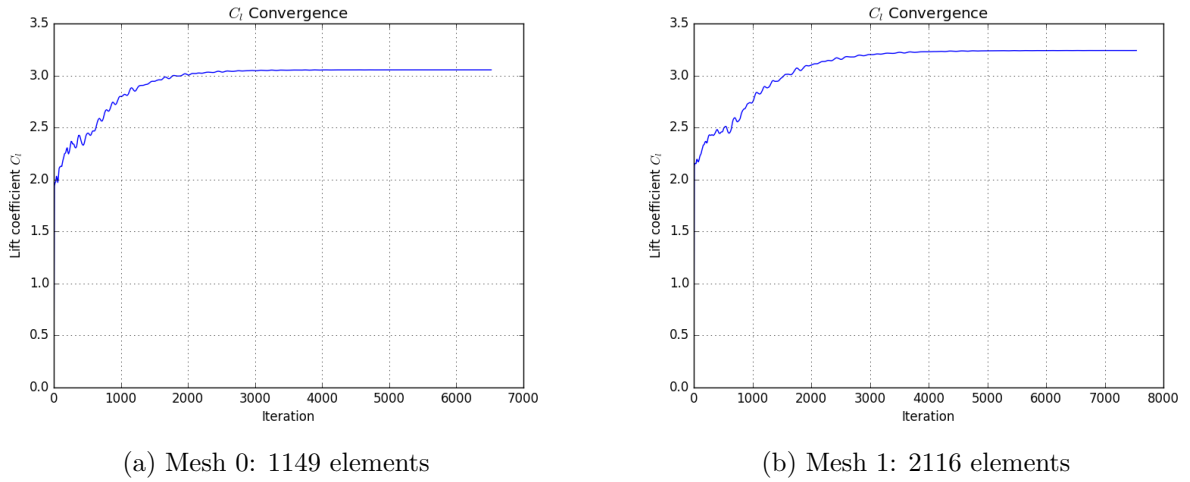


fig. 9: Lift coefficient convergence for mesh 0 and mesh 1 with second-order finite volume method implementation.

4.2.2 The total C_l and C_d values

(a) mesh 0: 1149 elements				(b) mesh 1: 2116 elements				
	total	main	slat		total	main	slat	
C_l	3.0543	2.3174	0.1587	0.5781	3.2401	2.4217	0.1811	0.6379
C_d	0.0629	-0.1415	-0.1021	0.3065	0.0440	-0.1558	-0.1314	0.3313

Table 3: The lift and drag coefficient for mesh 0 and mesh 1 with second-order finite volume method implementation.

The difference of the lift and drag coefficient between two different meshes, again, will be discussed in this section. Compare to first-order scheme, lift coefficient increases remarkably, peak at 3.0543 for mesh 0, and 3.2401 for mesh 1. And for drag coefficient, both meshes have lower values; similarly, flap contributes the most part of the drag and slat and main elements contribute the negative drag coefficient. Overall, second-order scheme gives a higher L over D value than first-order.

4.2.3 The Mach and pressure contours

Unlike first-order method, the contours in second-order have gone through the linear variate process, which interpolate the data between grids and grids to make the contours look much smoother. For two meshes run, Mach number contours reveal that there are two accelerating points, one is at the front of the leading edge of the main part, another is the leading edge of the flap.

Pressure contours, shown in Figure 11, testify the results of the mesh contours: two low pressure regions are locating at the leading edge of main and slat elements. A very high pressure spot at the leading edge of the slat indicates the spot of the stagnation point.

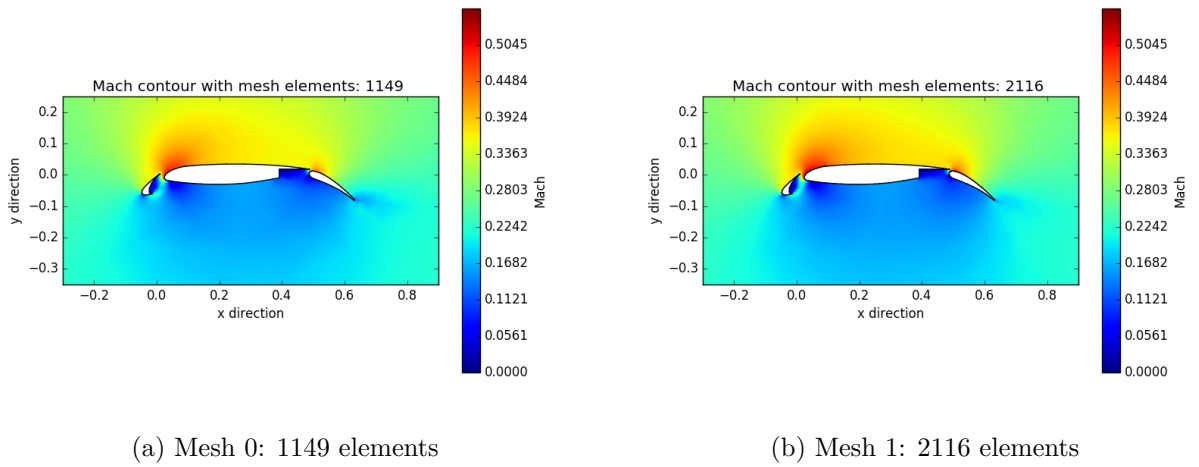


fig. 10: Mach number contour for mesh 0 and mesh 1.

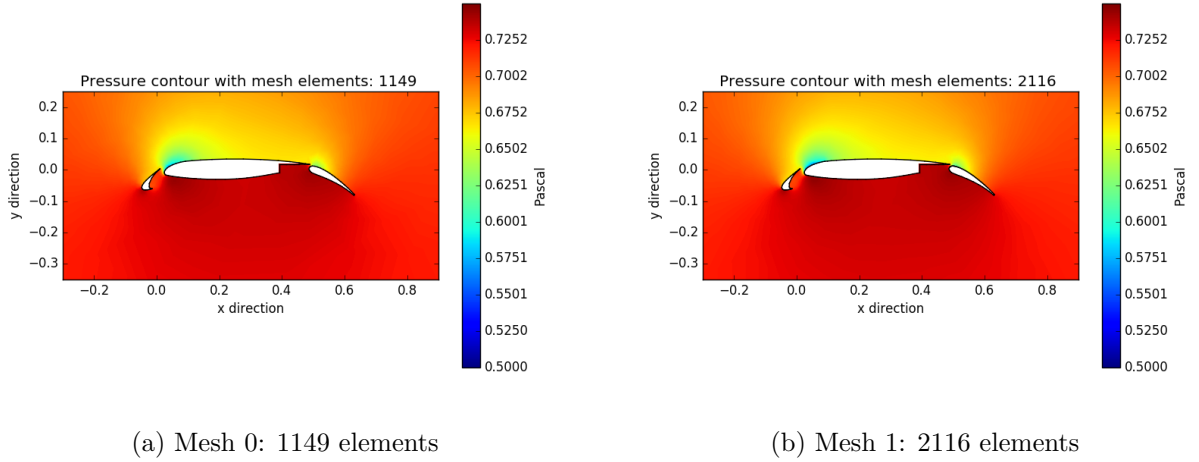


fig. 11: Pressure contour for mesh 0 and mesh 1.

4.2.4 The surface pressure coefficient, C_p , distribution

Unlike first-order method, second-order scheme gives mesh 0 and mesh 1 a more similar pressure coefficient distribution. Figure 12 shows that the pinnacle of the pressure coefficient is at the leading edge of the main elements, both meshes gives a very close number(about-5). The second highest spot is at the leading edge of the flap, however, mesh 1 gives the value of it around -4, but mesh 0 gives that around -3.

4.3 Plot the streamlines and calculate the mass flow rate in the slat/main and main/flap gaps.

Same as section 3.3, mass flow rate and streamline contours for second-order finite volume method are shown in this section, Table 4 and Figure 13, respectively. Unlike first-order finite volume method, the streamline contours result from second-order scheme shows that there are more streamlines flow through the gap between slat and main elements. This conclusion can also be testified by the data in Table 2 and Table 4, the mass flow rate derived from second-

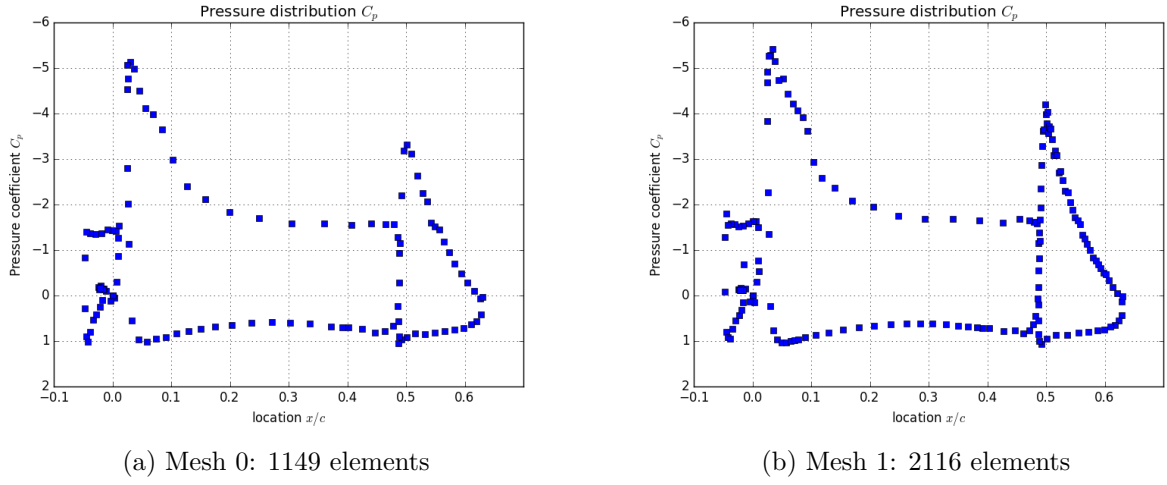


fig. 12: Pressure Coefficient(C_p) contour for mesh 0 and mesh 1.

order is about twice of that of first-order. In addition, it is clear to see that there is a blank space at the left side upper corner for both meshes, this is due to the plotting setting: the stream function limits setting is between -0.1 and 0.1 with 50 levels. Therefore, if any value of the stream function is higher than 0.1 or lower than -0.1 will not be shown.

(a) mesh 0: 1149 elements		(b) mesh 1: 2116 elements	
gap location	mass flow rate	gap location	mass flow rate
slap/main	0.006404	slap/main	0.006582
flap/main	0.002313	flap/main	0.002496

Table 4: Mass flow rate between the main/slap, main/flap gaps, for mesh 0 and mesh 1.

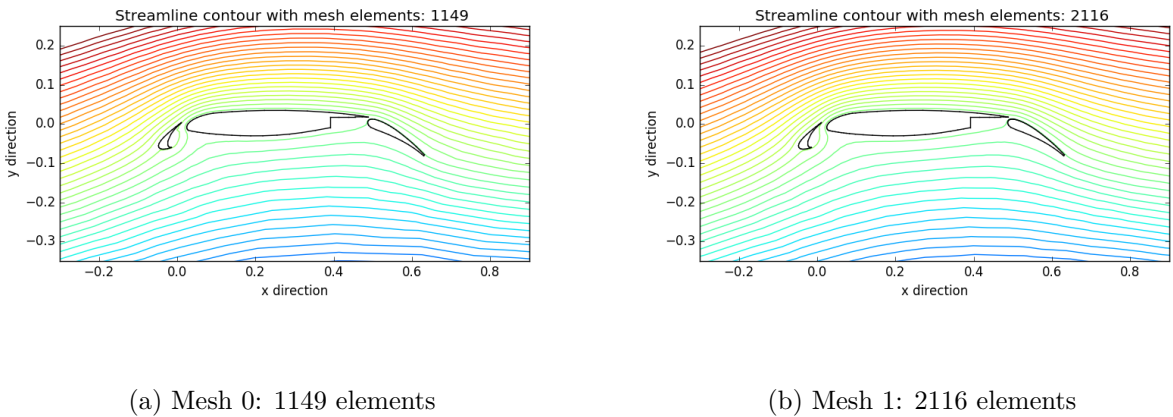


fig. 13: Streamline contour for mesh 0 and mesh 1.

5 More Dense Meshes: Mesh 2 and Mesh 3

In this section, more comparison between first-order and second-order schemes applied on higher resolution meshes will be discussed. The results will be shown in two subsections, mesh 2 with first and second-order finite volume method, and, mesh 3 with both methods.

5.1 Mesh 2: 4124 elements

5.1.1 Residuals and C_l convergence with iterations

Figures 14 shows the residual convergence versus iterations. For second-order method, it requires more than two times iterations than it needs for first-order method to converge to the tolerance. Also, the magnitude of the oscillation of second-order scheme is smaller than first-order. This indicates that higher-order scheme has less discrepancy between aligned iterations.

In addition to residual convergence, Figure 15 gives the lift coefficient convergence versus iterations. From lift convergence graph, the oscillation magnitude between high order and low order scheme is even more clear. Although both schemes give a stable C_l value after 3000 iterations, the convergent value and the oscillation pattern before 3000 iterations are quite different. As we can see, the convergent value of C_l for first-order is about 2.3 and for second-order is about 3.3, there are around 1.0 difference. For the magnitude of oscillation, first-order has a large difference between one iteration and another, the highest difference is almost 2.0 at the iteration about 300. On the other hand, second-order has a smaller oscillation and the C_l value climbs steadily and peak at 3.3 roughly.

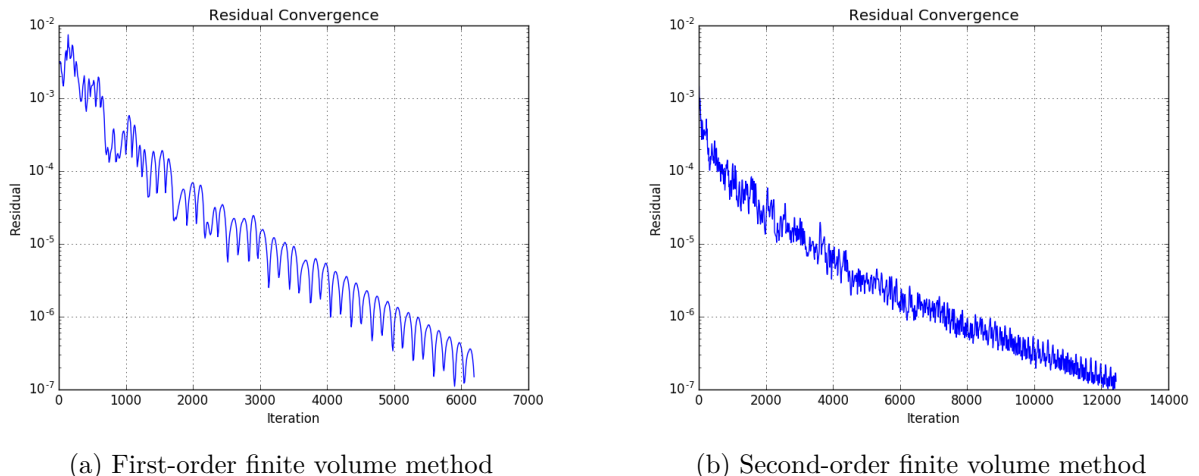


fig. 14: Residual convergence for first and second-order method for mesh 2.

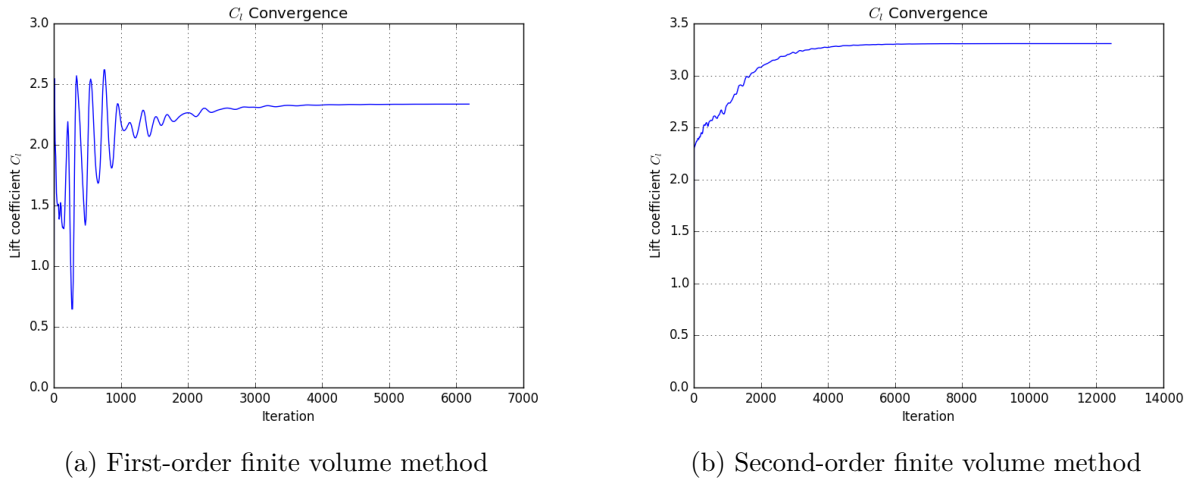


fig. 15: Lift coefficient convergence for first and second-order method for mesh 2.

5.1.2 The Mach and pressure contours

For both Mach and pressure contours, the results from second-order tend to give more subtle difference between grids and grids. For example, from second-order Mach number contour, high Mach number, greater than 0.48, region limited to only the leading edge of main and flap parts, unlike first-order method, the whole region above the main wing element are marked as high Mach number, 0.35. Pressure contours also reflects this fact: the contour result from second-order scheme has more different colour distribution in certain area, above or below the airfoil, than that from first-order. Instead of showing the discrete data contours, linear variation processed graphs are shown in the Appendix.

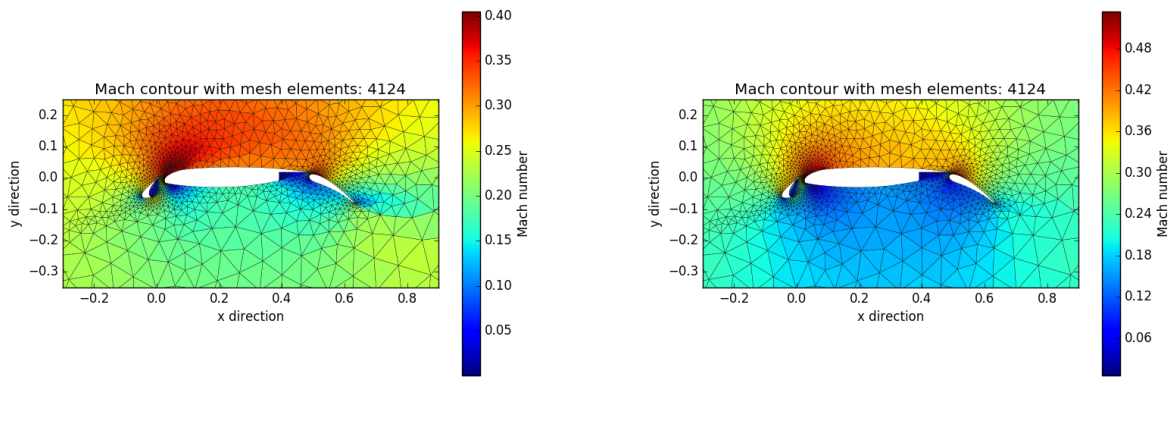


fig. 16: Mach contours for first and second-order method for mesh 2.

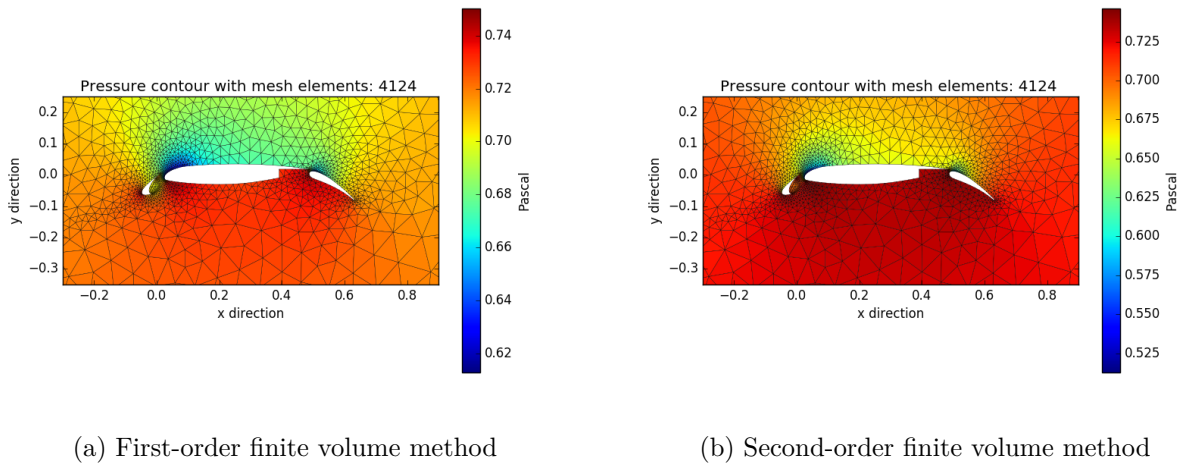


fig. 17: Pressure contours for first and second-order method for mesh 2.

5.1.3 The surface pressure coefficient distribution

The difference between first-order and second-order is remarkable. The lowest point of the C_p value on the upper surface of the airfoil result from second-order, is about -6.0, but for first-order, that is only a half of it, about -3.0.

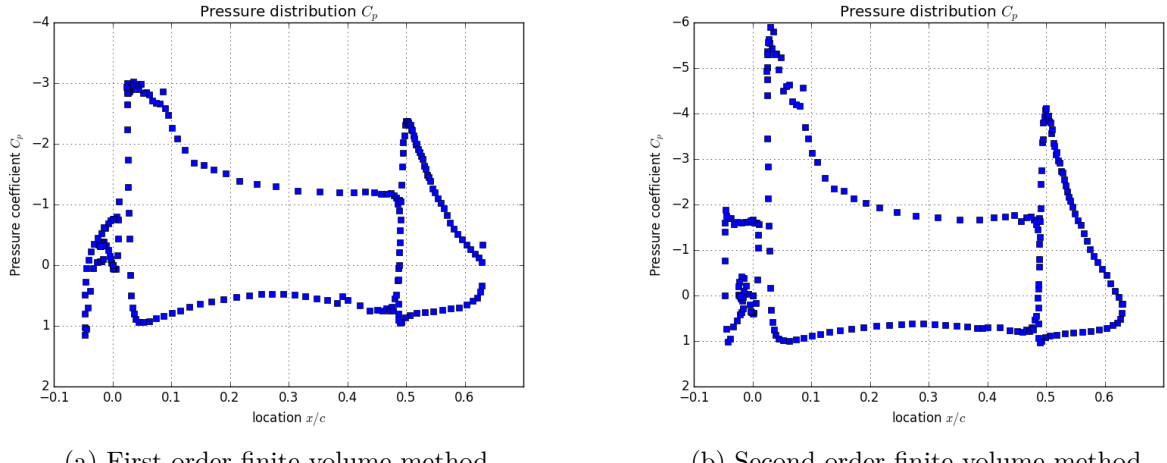


fig. 18: Pressure Coefficient(C_p) contours for first and second-order method for mesh 2.

5.1.4 The C_l and C_d values

Both lift and drag coefficients give a more direct and comparable base for first and second-order method. Though both methods indicate that the dominator of the lift is the main wing element, drag is the flap element, the corresponding values are having considerable difference. For total C_l , second-order method gives almost 1.0 higher value than first-order, and for C_l contributed from the slat are even having about 3 times difference. Moreover, the total C_d value given by second-order scheme is just roughly one-tenth of that given by first-order.

(a) First-order finite volume method

	total	main	slat	flap
C_l	2.3358	1.8048	0.0557	0.4753
C_d	0.2268	-0.0647	0.0185	0.2729

(b) Second-order finite volume method

	total	main	slat	flap
C_l	3.3066	2.4731	0.1839	0.6495
C_d	0.0266	-0.1711	-0.1386	0.3363

Table 5: The lift and drag coefficient for first and second-order finite volume method for mesh 2.

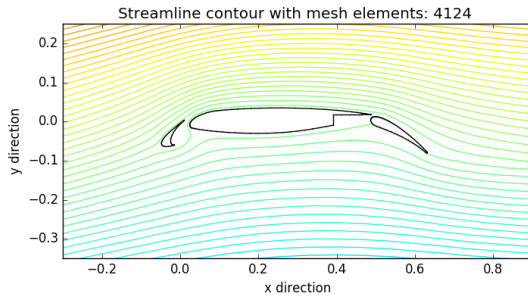
5.1.5 Plot the streamlines and calculate the mass flow rate in the slat/main and main/flap gaps.

Unlike lift and drag coefficients, the mass flow rate and streamline contours calculated from first and second-order schemes looks similar at first, but some subtle differences still exist. Although the difference of the mass flow rate between main/slat gap is just around 0.002, it is also around 33 percent difference. For streamline contours, it is clear to see that the streamlines, result from second-order method, in the front of the airfoil have more distortion than the streamlines result from first-order method.

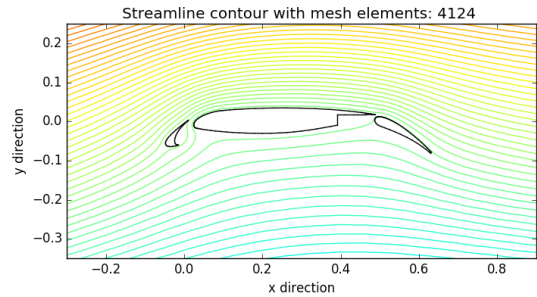
(a) First-order finite volume method	
gap location	mass flow rate
slap/main	0.004852
flap/main	0.001960

(b) Second-order finite volume method	
gap location	mass flow rate
slap/main	0.006886
flap/main	0.002494

Table 6: Mass flow rate between the main/slap, main/flap gaps, for first and second-order scheme for mesh 2.



(a) First-order finite volume method



(b) Second-order finite volume method

fig. 19: Streamline contours for first and second-order method for mesh 2.

5.2 Mesh 3: 8031 elements

5.2.1 Residuals and C_l convergence with iterations

Similarly, residual and lift coefficient convergence plots indicate that the second-order method needs more iterations to converge: around 8000 and 17000 iterations, respectively. Furthermore, with more iterations, it requires much more running time to converge: 2.5 hours

for first-order, 15.8 hours for second-order. Additionally, along with higher iterations, the oscillation pattern of residual convergence becomes more periodically.

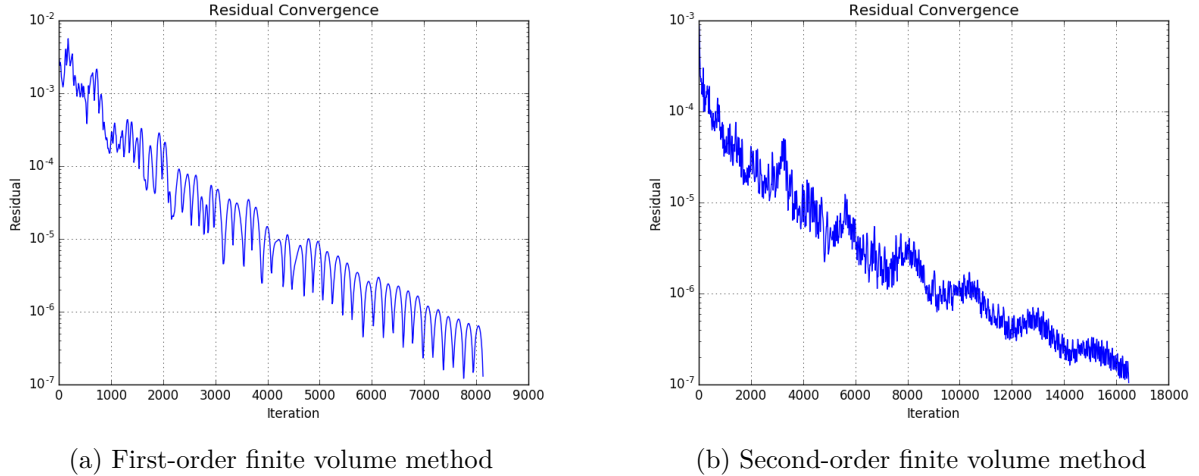


fig. 20: Residual convergence for first and second-order method for mesh 3.

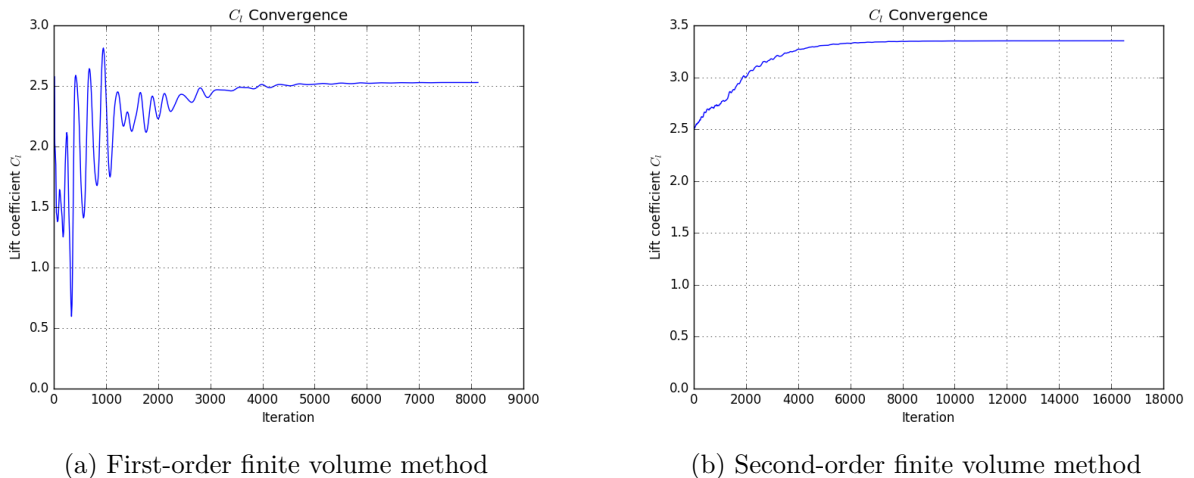
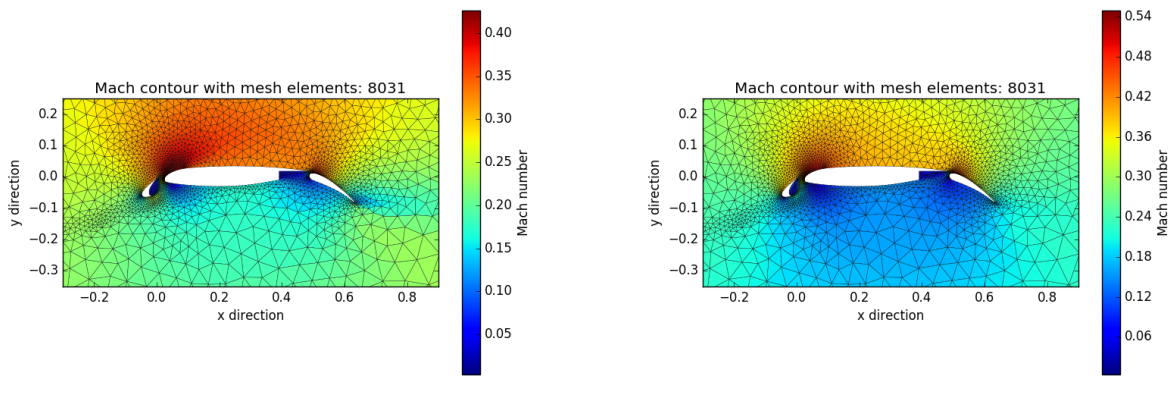


fig. 21: Lift coefficient convergence for first and second-order method for mesh 3.

5.2.2 The Mach and pressure contours

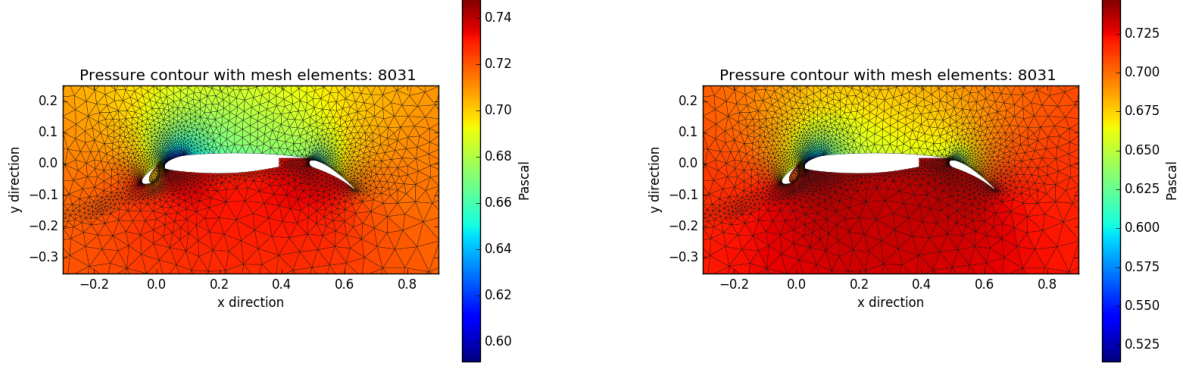
Just like the discussion in section 5.1, second-order method gives more subtle velocity and pressure distribution in the contour graph. Besides, a remarkable difference between first and second-order result is the range of Mach number. From the colour bar in Figure 22 and 23, we can find that the highest Mach number in second-order is .54, and in first-order is only .40, which is about 25 percent increase. Recall the free stream Mach number is just .25. However, for pressure contour, the difference between first and second-order is not that significantly.



(a) First-order finite volume method

(b) Second-order finite volume method

fig. 22: Mach contours for first and second-order method for mesh 3.



(a) First-order finite volume method

(b) Second-order finite volume method

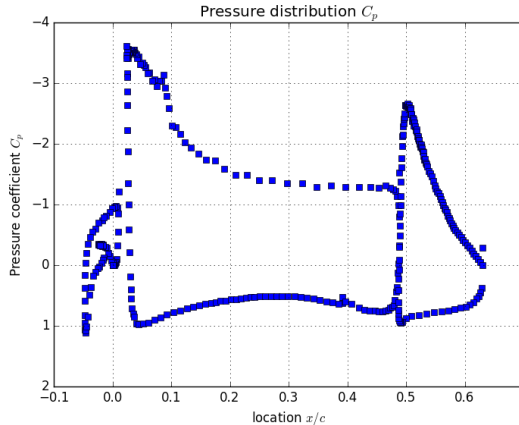
fig. 23: Pressure contours for first and second-order method for mesh 3.

5.2.3 The surface pressure coefficient distribution

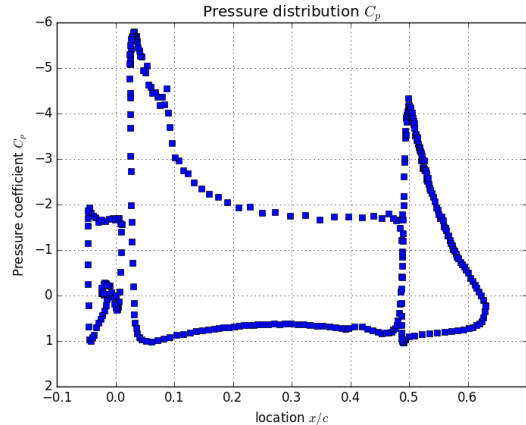
Figure 24 shows the coefficient of pressure. It is clear to see that, first-order method result has few data with large displacement: the point at the rear of the airfoil. On the other hand, the first-order method tends to give a more curve, smooth pressure distribution at the leading edge; second-order tends to gives a more abrupt result at that point. In reality, leading edge is near the stagnation point, at this point, the flow velocity will be zero, and cause a high pressure. Therefore, abrupt pressure distribution could be more reality accordance.

5.2.4 The C_l and C_d values

Table 7 shows the C_l and C_d for mesh 3 with first and second-order method. As the densest grid, both method give the highest lift coefficient and lowest drag coefficient among all the meshes run. However, between both methods, there are still about 0.8 difference in C_l and ten times difference in C_d . In reality, drag can be separated into 3 parts, pressure drag, friction drag and wave drag. Therefore, compare to lift force, drag force is usually hard to be predicted.



(a) First-order finite volume method



(b) Second-order finite volume method

fig. 24: Pressure Coefficient(C_p) contours for first and second-order method for mesh 3.

Though here only the pressure drag will be considered(inviscid, low Mach number flow), the drag coefficient rely on pressure at four different locations, leading edge, trailing edge, slat/main gap and main/flap gap. Compare to only two data(upper surface and lower surface) for lift coefficient, four data for drag coefficient tend to lead a higher error.

(a) First-order finite volume method

	total	main	slat	flap
C_l	2.5284	1.9428	0.0794	0.5062
C_d	0.1892	-0.0901	-0.0339	0.2832

(b) Second-order finite volume method

	total	main	slat	flap
C_l	3.3513	2.5014	0.1903	0.6596
C_d	0.0190	-0.1733	-0.1486	0.3409

Table 7: The lift and drag coefficient for first and second-order finite volume method for mesh 3.

5.2.5 Plot the streamlines and calculate the mass flow rate in the slat/main and main/flap gaps.

Table 8 and Figure 25 show the mass flow rate between slat/main and main/flap gaps and streamline contour, respectively. Unlike the graph in section 4, there is no blank at the left side upper corner. Here, the stream function limits setting has been changed from -0.2 to 0.2 with 100 levels. The streamline density remain unchanged, but more data can be shown in the graph.

(a) First-order finite volume method

gap location	mass flow rate
slap/main	0.005375
flap/main	0.002045

(b) Second-order finite volume method

gap location	mass flow rate
slap/main	0.006872
flap/main	0.002516

Table 8: Mass flow rate between the main/slap, main/flap gaps, for first and second-order scheme for mesh 3.

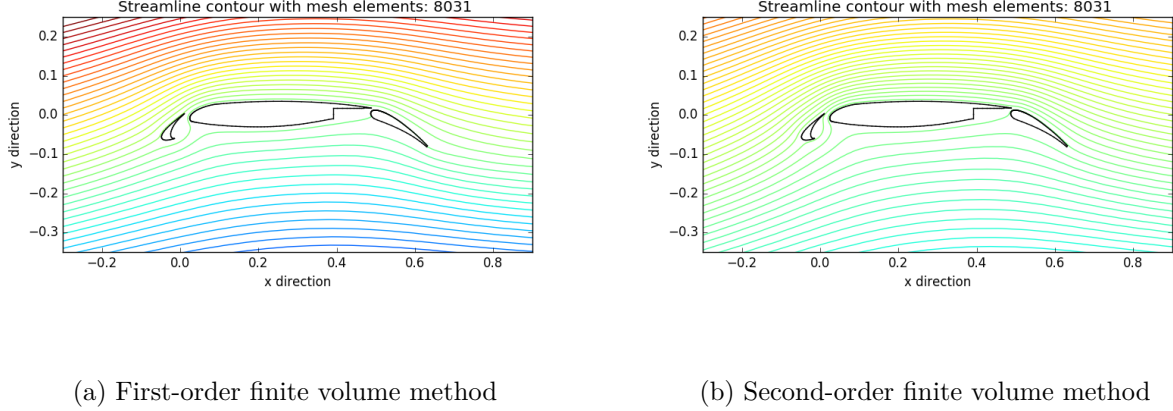


fig. 25: Streamline contours for first and second-order method for mesh 3.

6 Conclusion

This project shows the difference between first-order and second-order finite volume methods, and the differences between fine and coarse meshes. And the case is based on an airfoil with high-lift devices: slat and flap.

In first-order finite volume method, every mesh is able to converge less than 9000 iterations and 2.5 hours. However, the converged solutions are not accurate enough. Lift coefficients are too low for an airfoil with high-lift devices.[2] On the other hand, the drag coefficient is too high. But we should remain a conservative attitude for it, since this project only consider inviscid flow - there is no viscous drag. However, a reasonable drag coefficient should be the order of 10^{-2} , which is ten times difference of the data given by first-order(even the finest mesh.)

In section 4, second-order finite volume method is implemented to solve the question. As the data show in Table 3, lift coefficient is higher than 3.0(coarsest mesh), which is higher than the C_l given by mesh 3 with first-order. For drag coefficient, mesh 0 with second-order is 0.063, is much lower and within an order of 10^{-2} .

In conclusion, the second-order scheme gives higher accuracy than first-order scheme, fine meshes gives higher accuracy than coarse meshes. However, for the mesh 0 with second-order method, the C_l is higher than mesh 3 with first-order, and the C_d is lower too. This fact gives us a reliable conclusion - increasing the order of a scheme gives more accuracy than increasing the mesh elements.

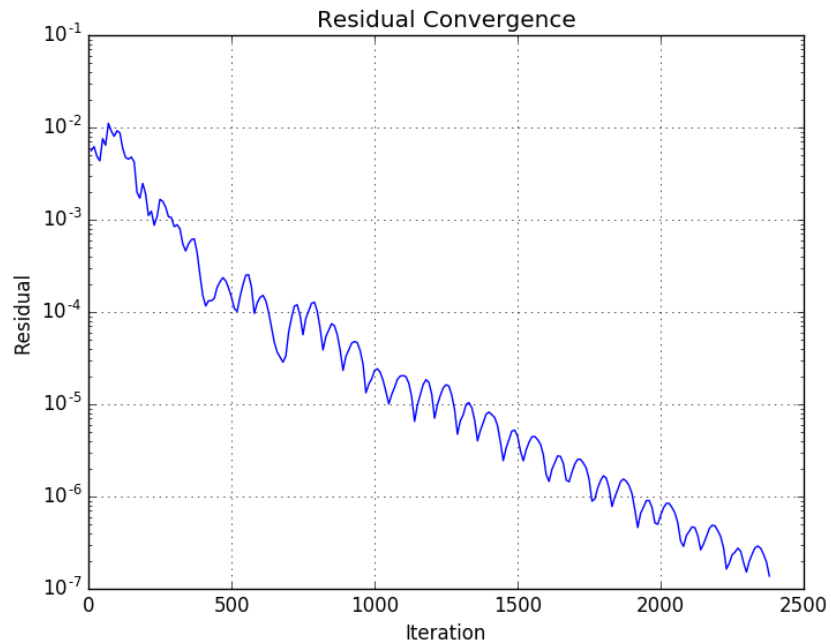
Reference

- [1] Hirsch,Charles: *Numerical Computation of Internal and External Flows, vol.I:Fundamentals of Numerical Discretization*, Wiley, New York, 1988.
- [2] John Anderson: *Fundamental of Aerodynamics*, McGraw-Hill 2007.

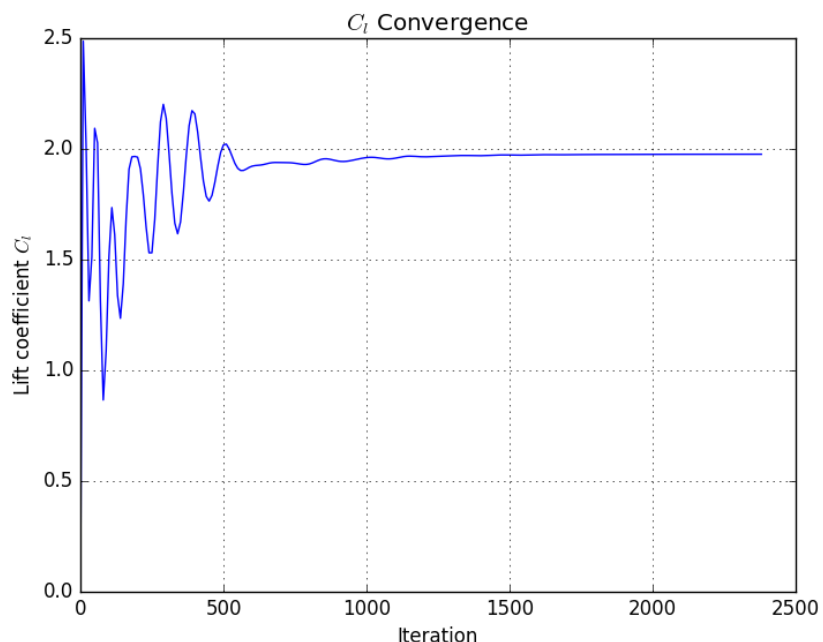
Appendix

First-order scheme

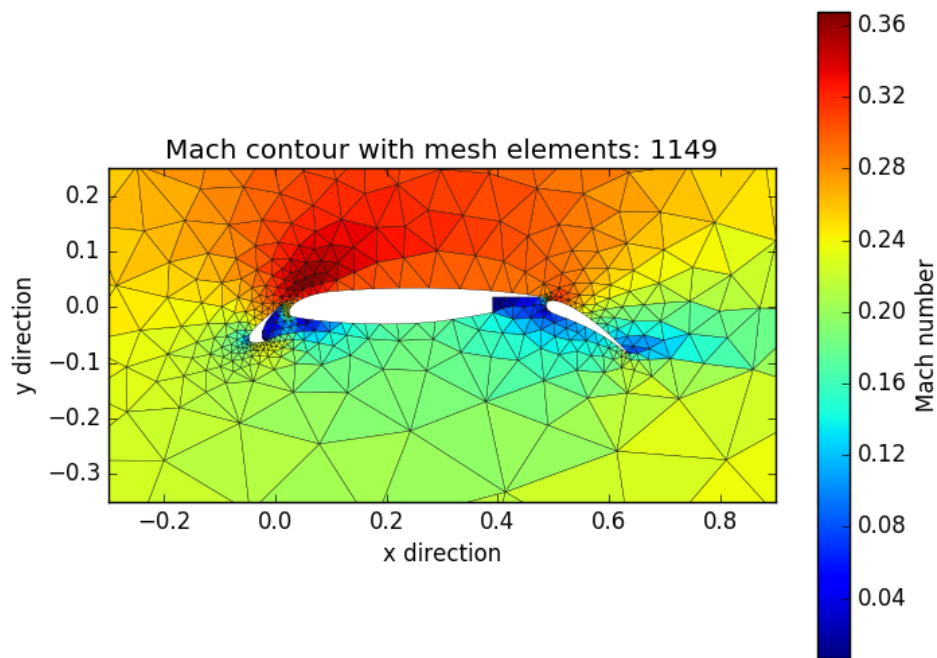
Mesh 0



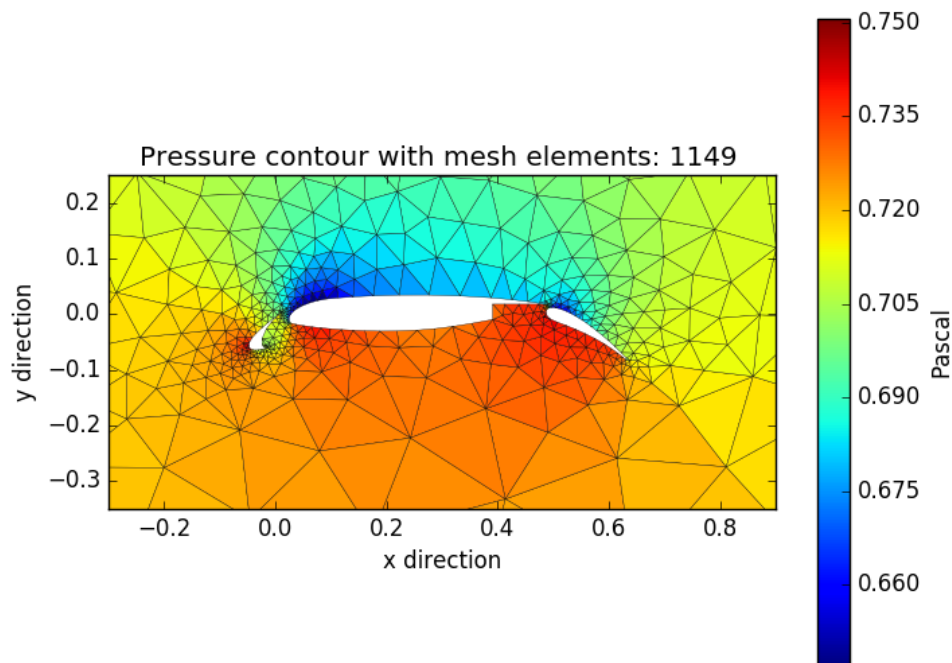
Residual for mesh 0, first-order method



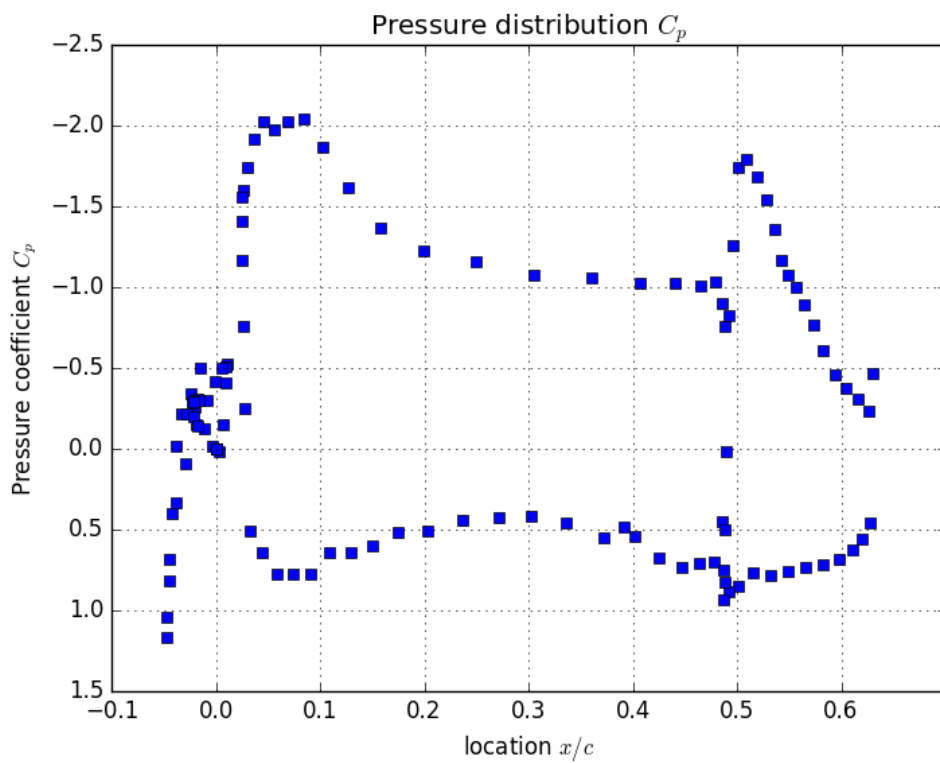
Lift coefficient for mesh 0, first-order method



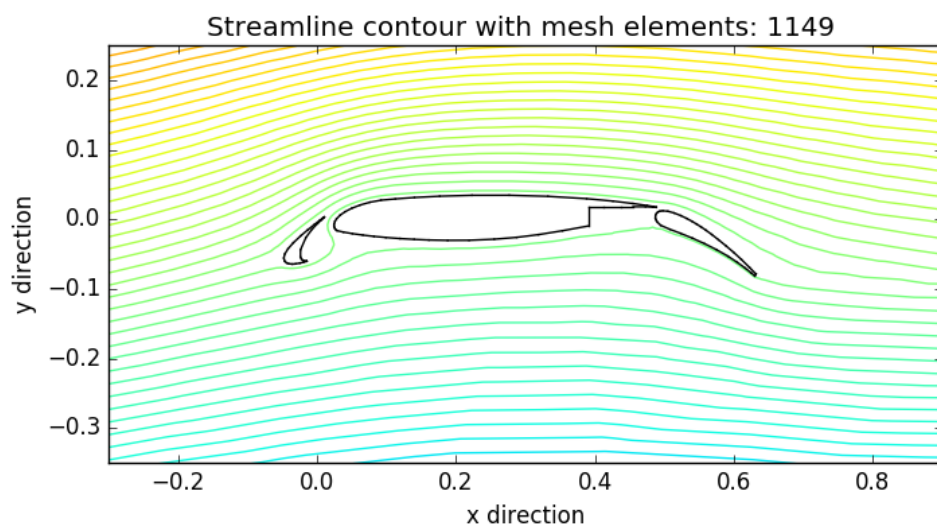
Mach contour for mesh 0, first-order method



Pressure contour for mesh 0, first-order method

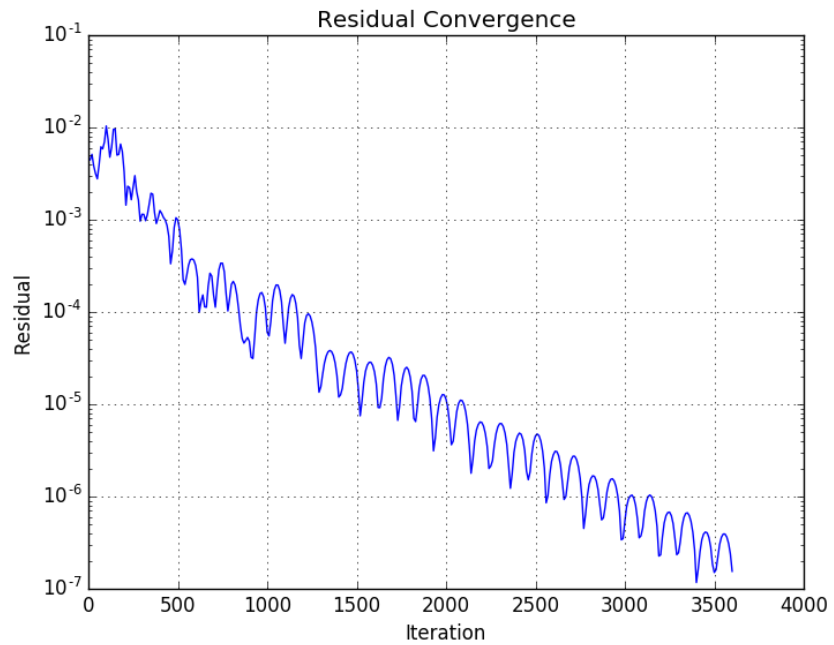


Pressure coefficient for mesh 0, first-order method

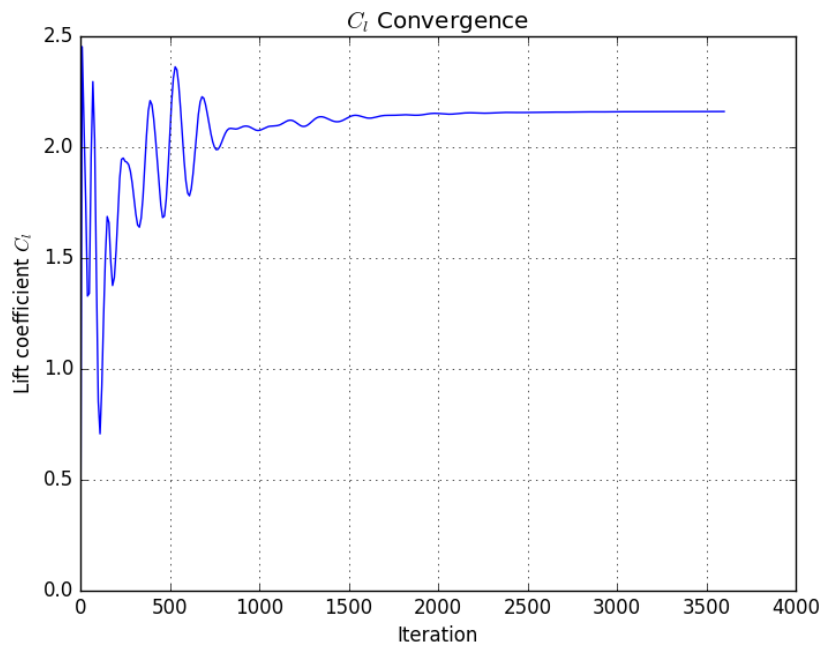


Streamline contour for mesh 0, first-order method

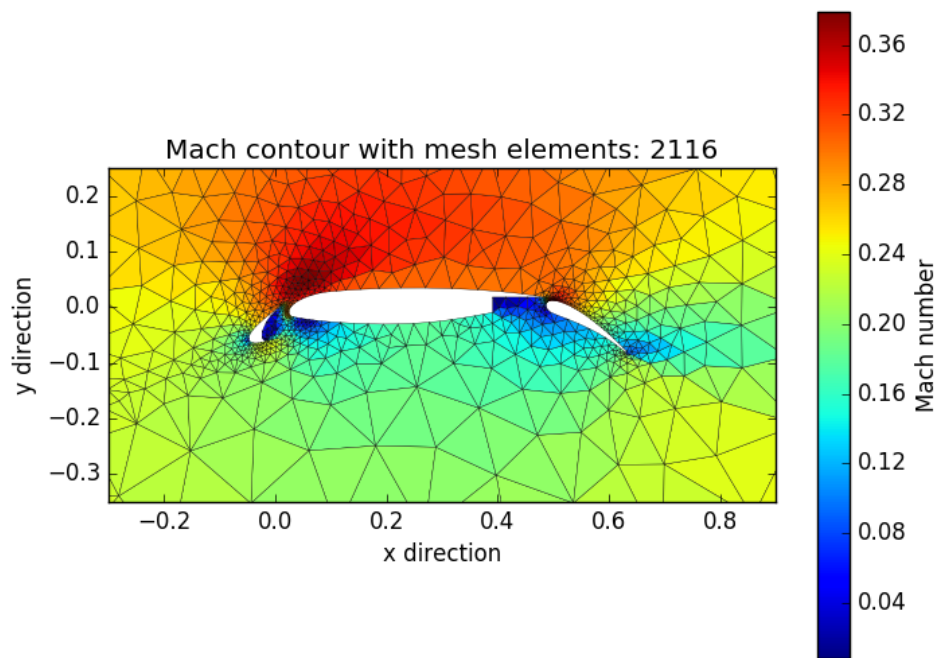
Mesh 1



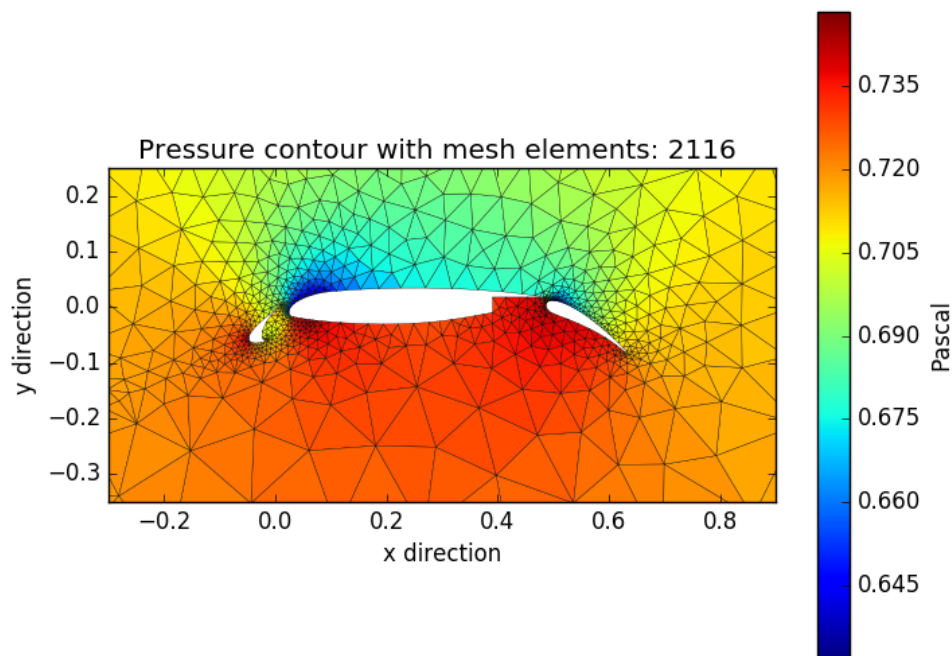
Residual for mesh 1, first-order method



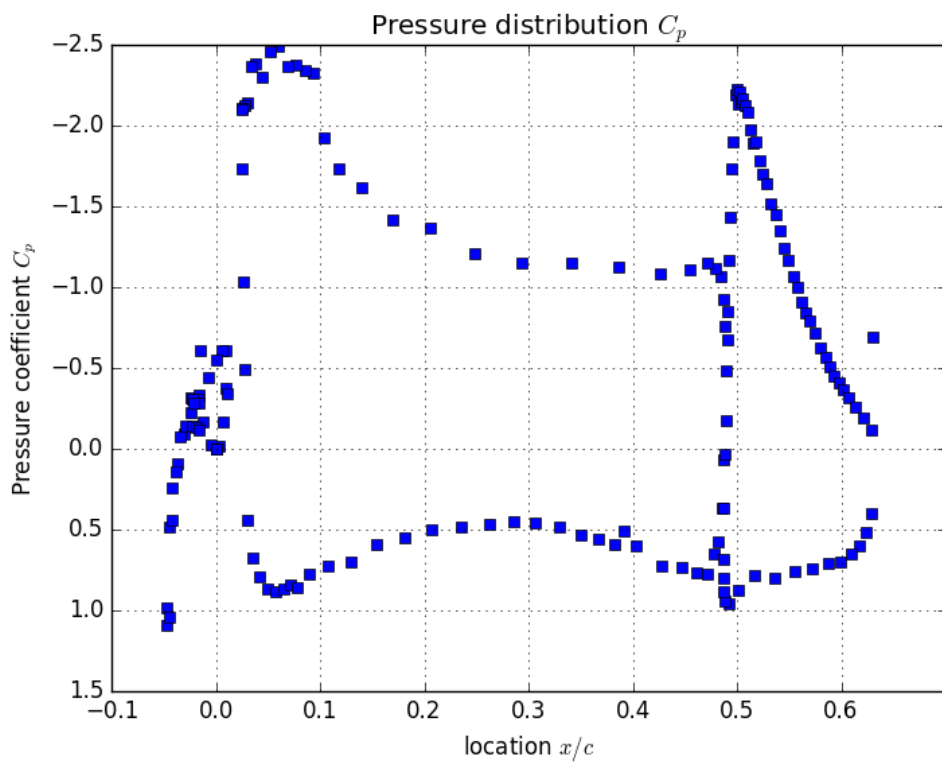
Lift coefficient for mesh 1, first-order method



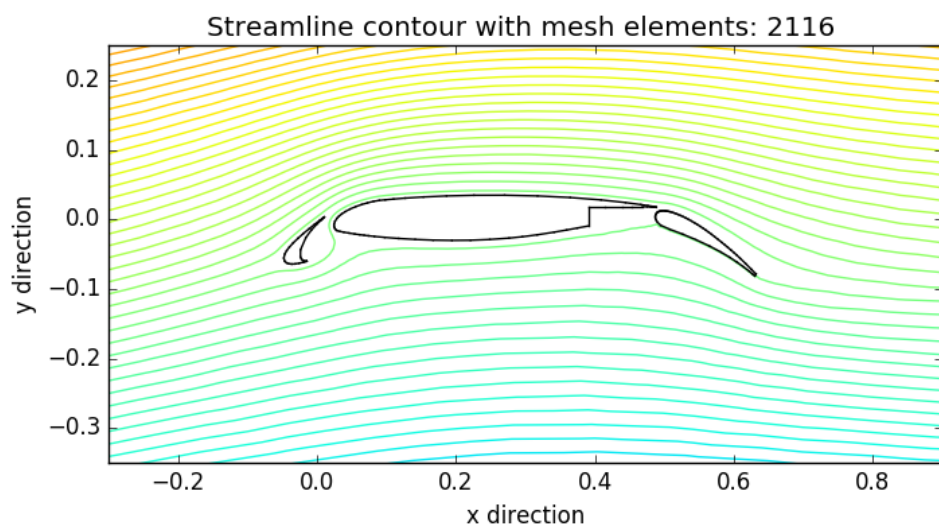
Mach contour for mesh 1, first-order method



Pressure contour for mesh 1, first-order method

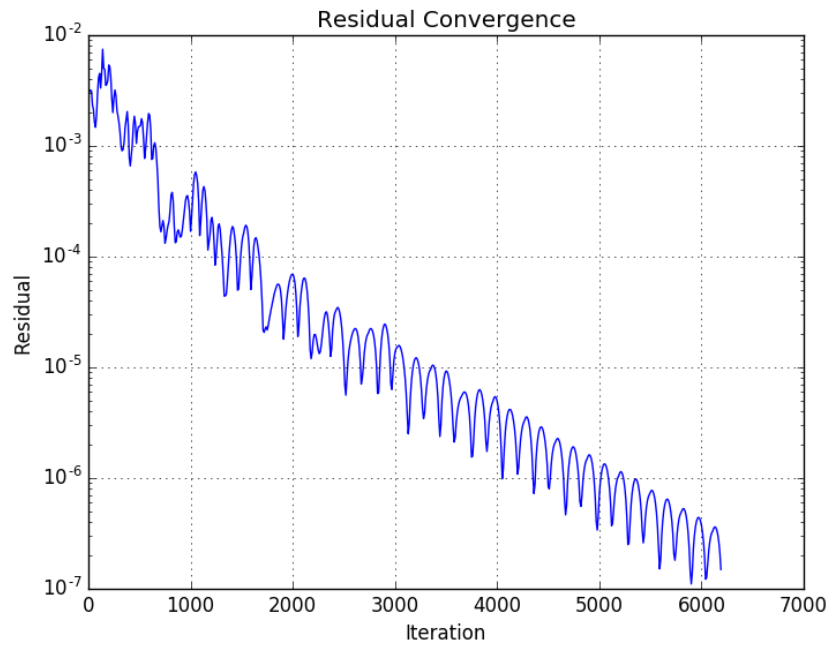


Pressure coefficient for mesh 1, first-order method

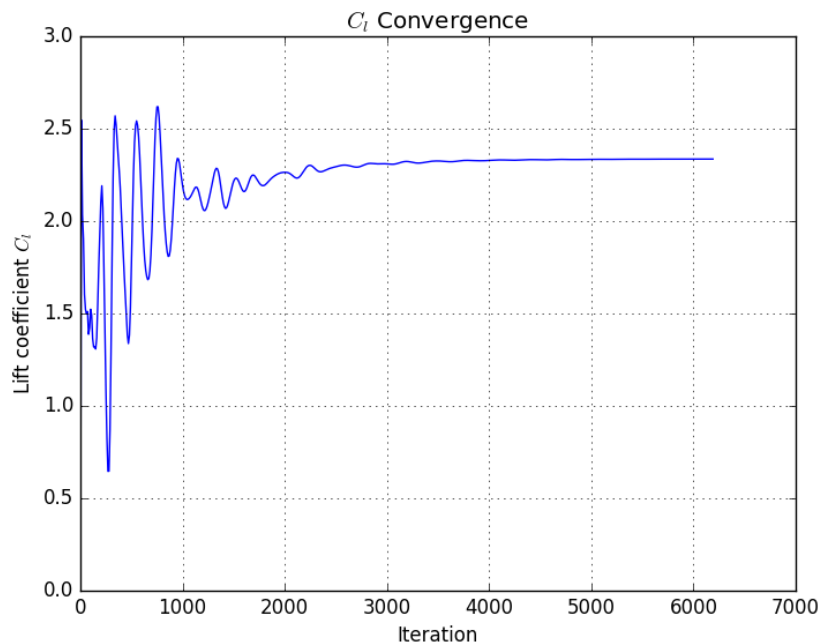


Streamline contour for mesh 1, first-order method

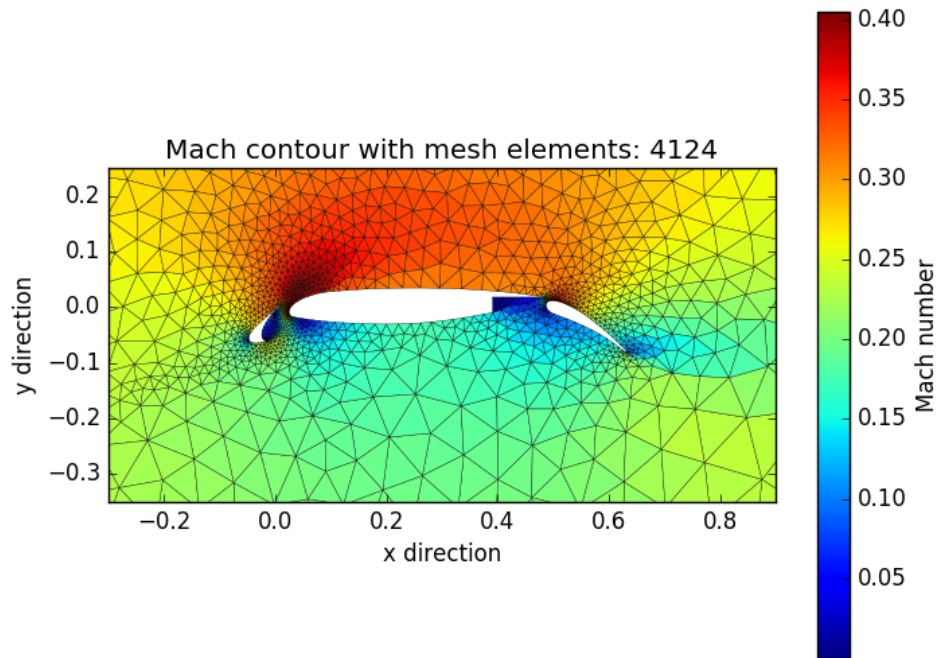
Mesh 2



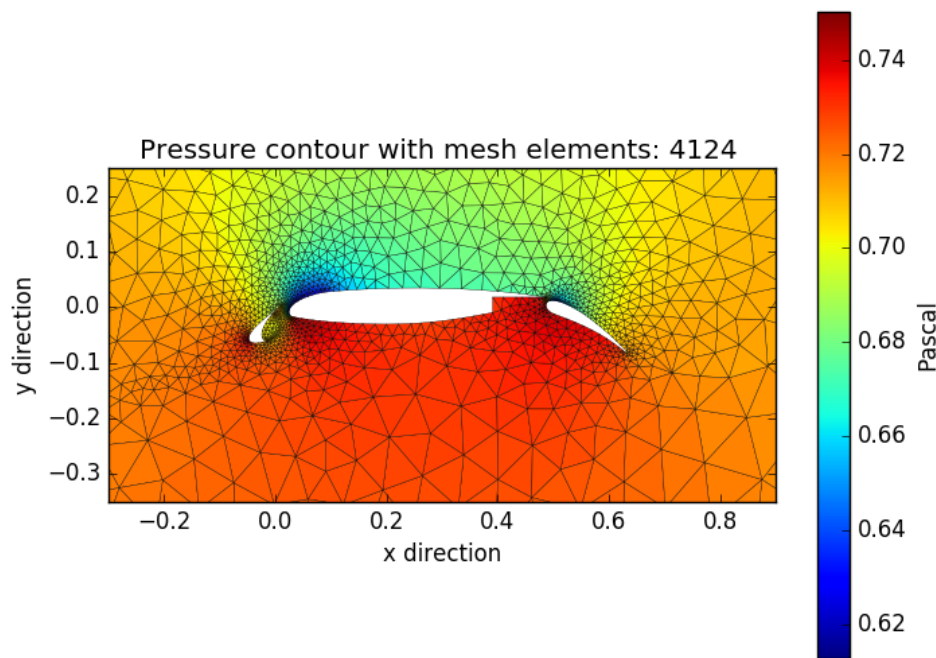
Residual for mesh 2, first-order method



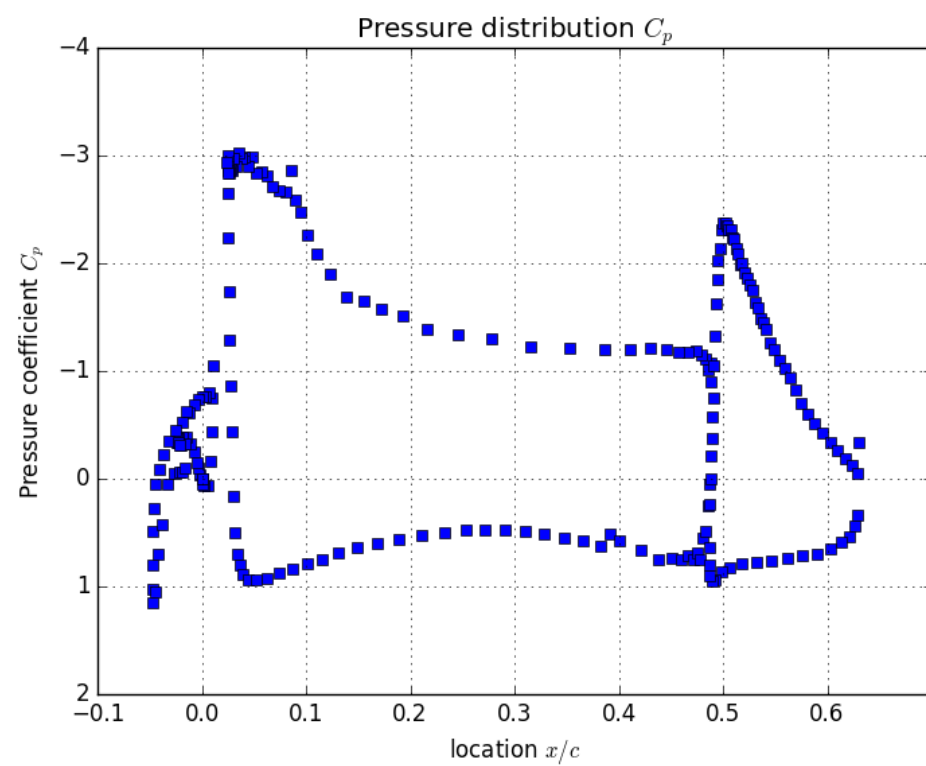
Lift coefficient for mesh 2, first-order method



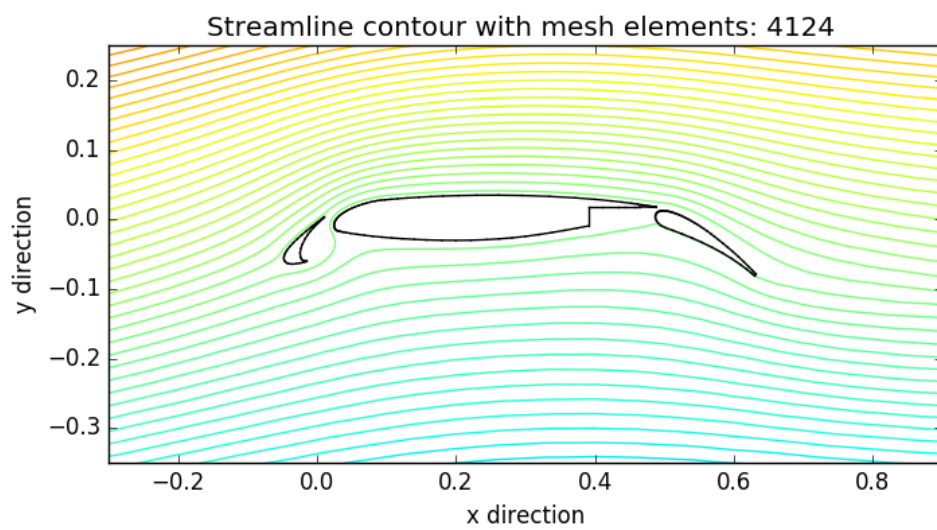
Mach contour for mesh 2, first-order method



Pressure contour for mesh 2, first-order method

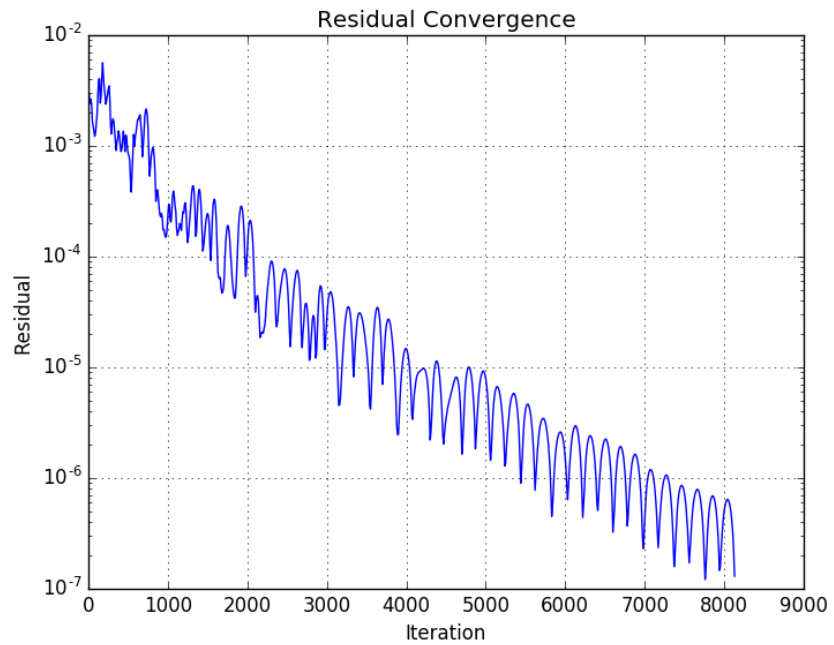


Pressure coefficient for mesh 2, first-order method

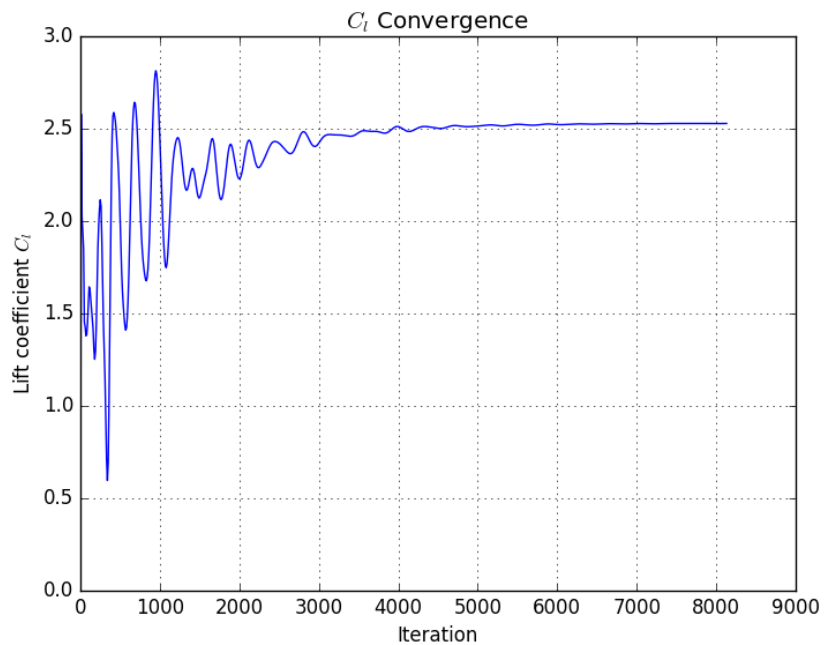


Streamline contour for mesh 2, first-order method

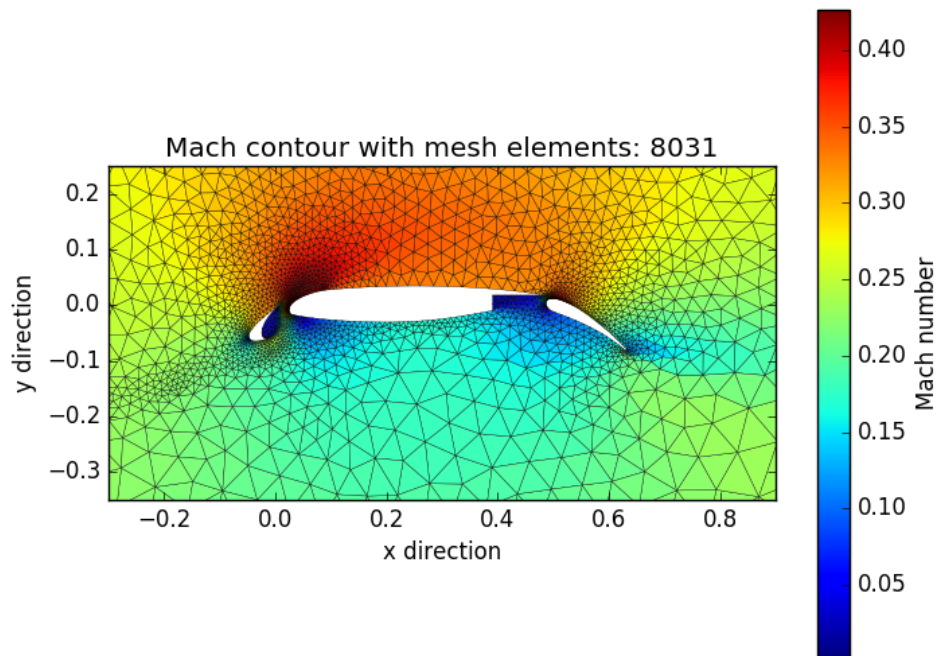
Mesh 3



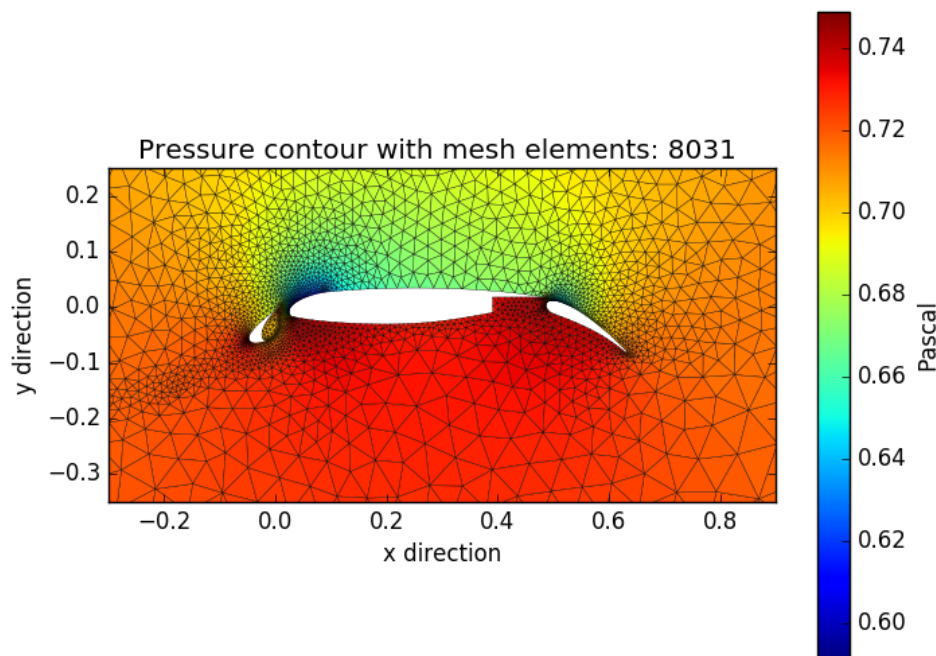
Residual for mesh 3, first-order method



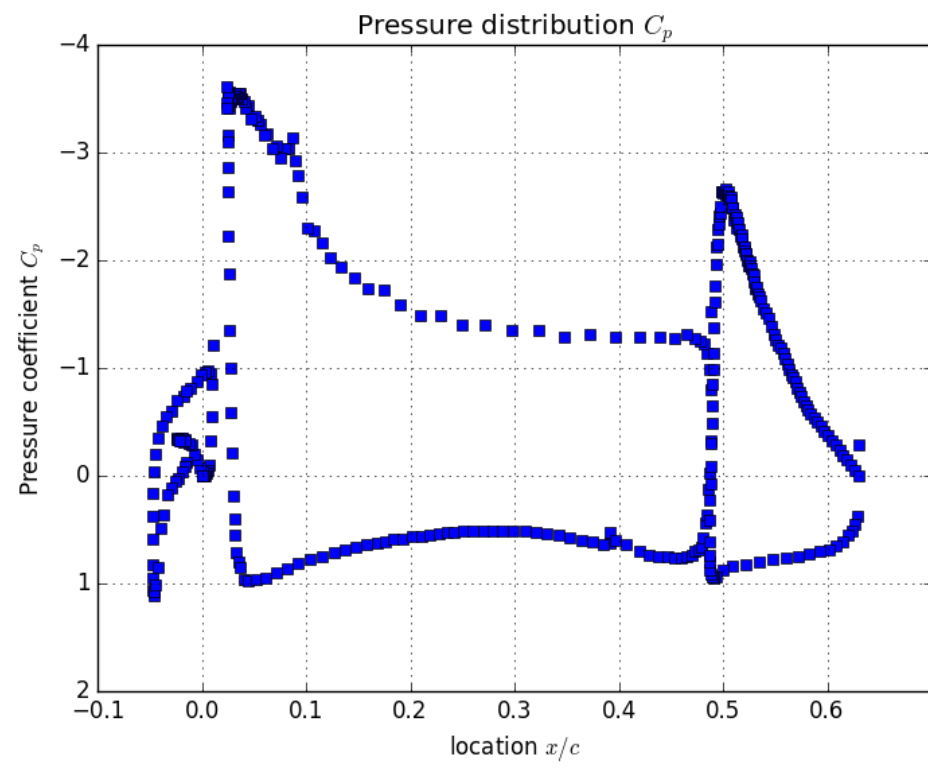
Lift coefficient for mesh 3, first-order method



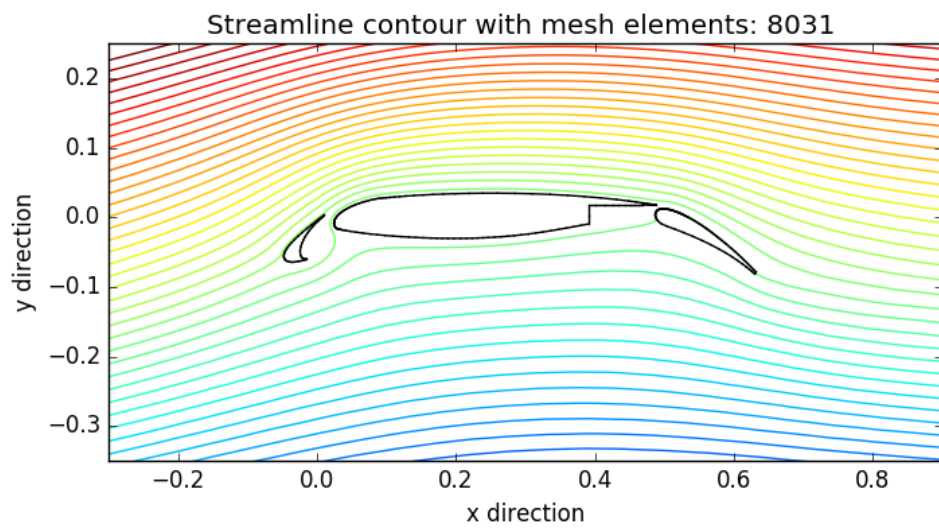
Mach contour for mesh 3, first-order method



Pressure contour for mesh 3, first-order method



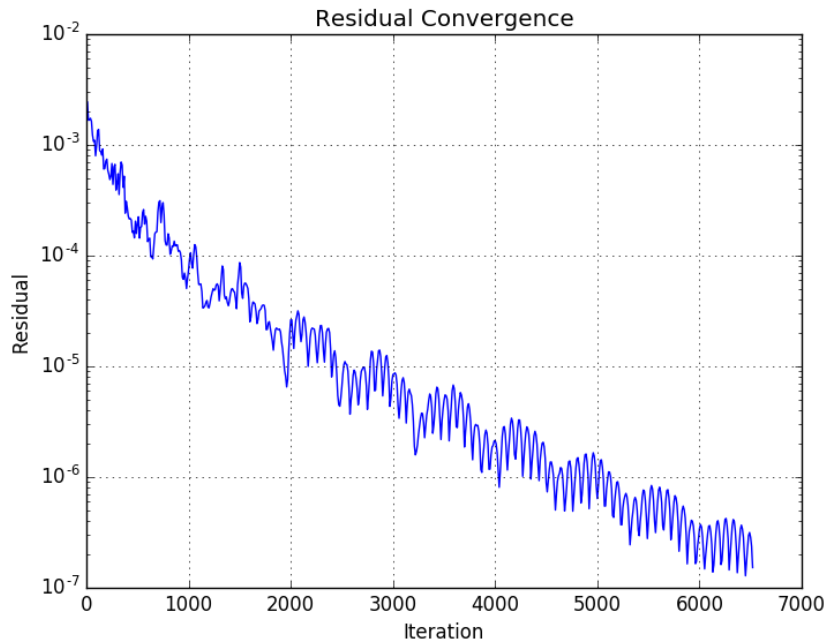
Pressure coefficient for mesh 3, first-order method



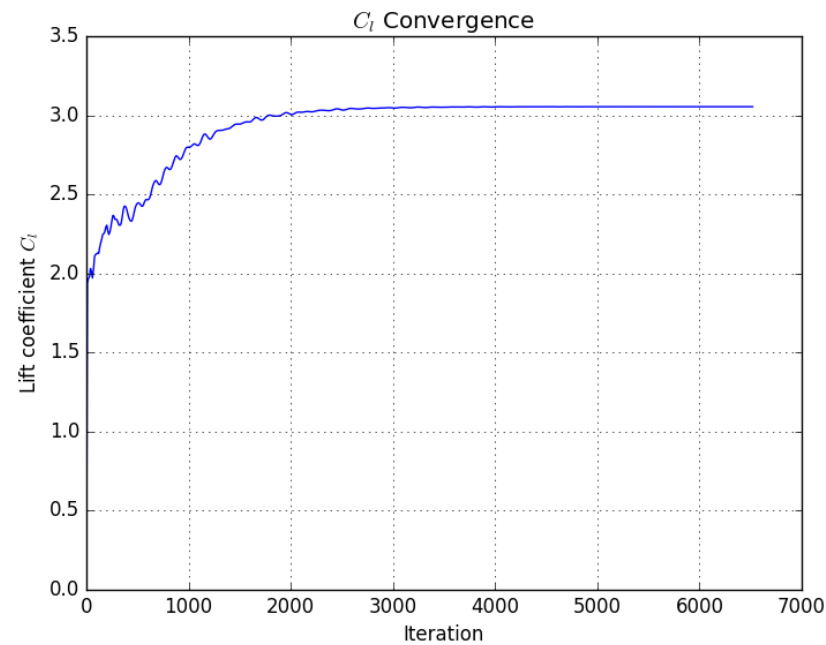
Streamline contour for mesh 3, first-order method

Second-order scheme

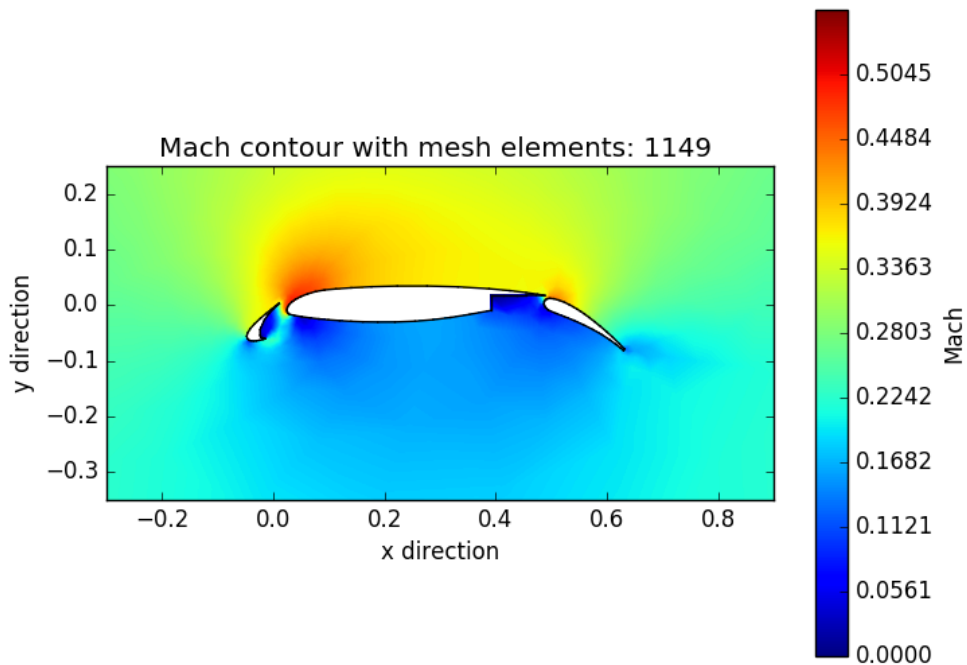
Mesh 0



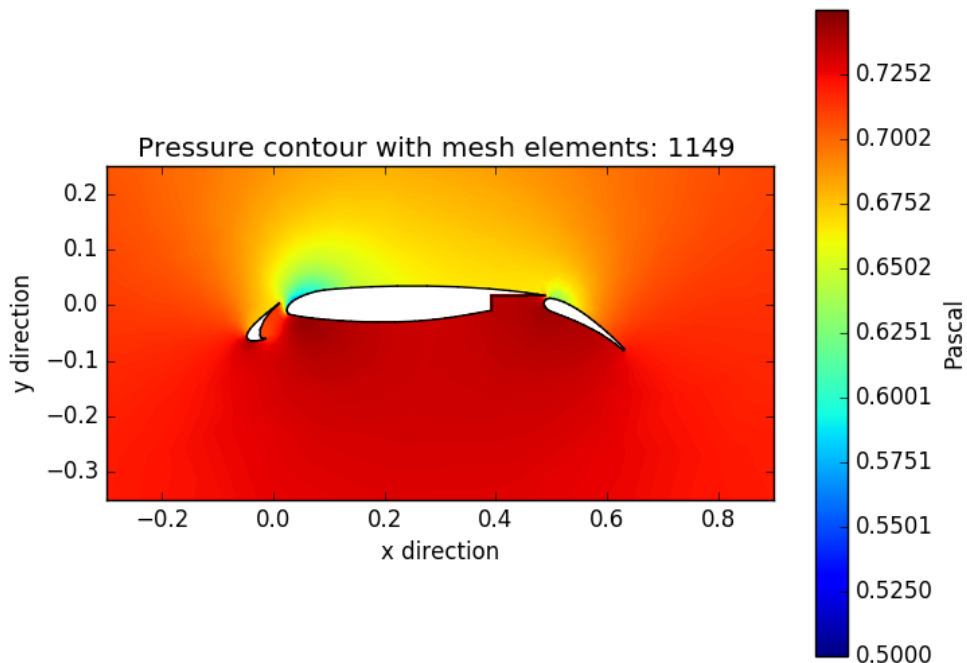
Residual for mesh 0, second-order method



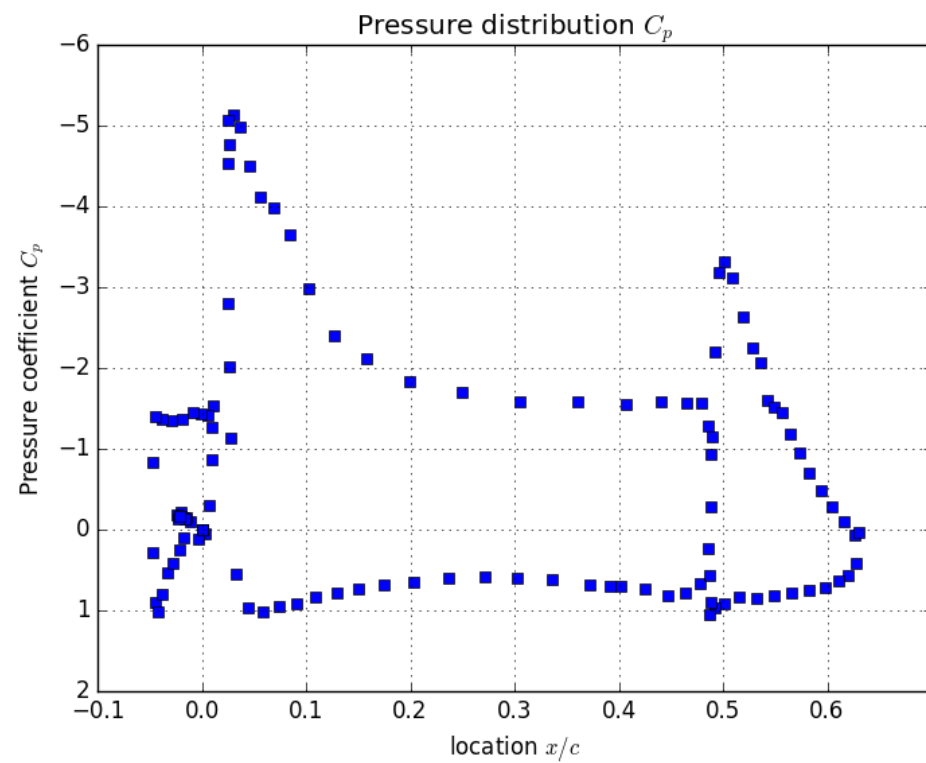
Lift coefficient for mesh 0, secondt-order method



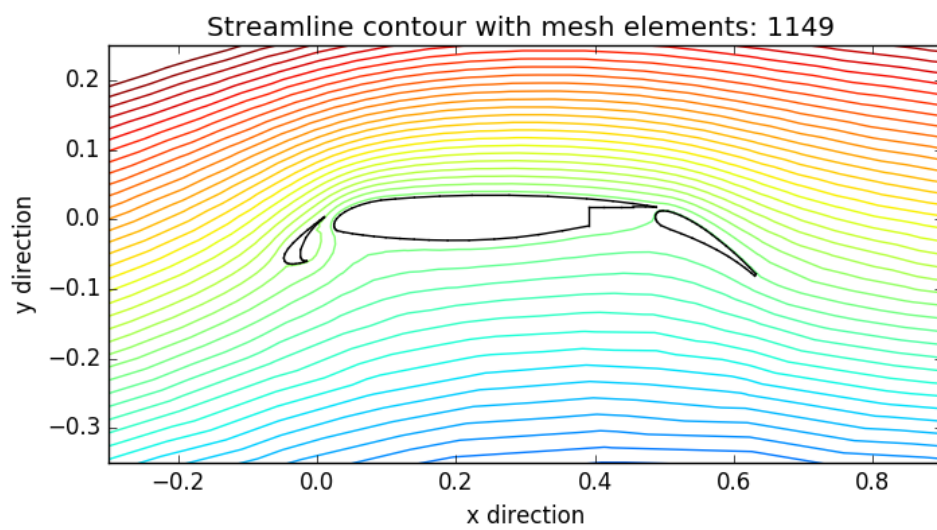
Mach contour for mesh 0, second-order method



Pressure contour for mesh 0, second-order method

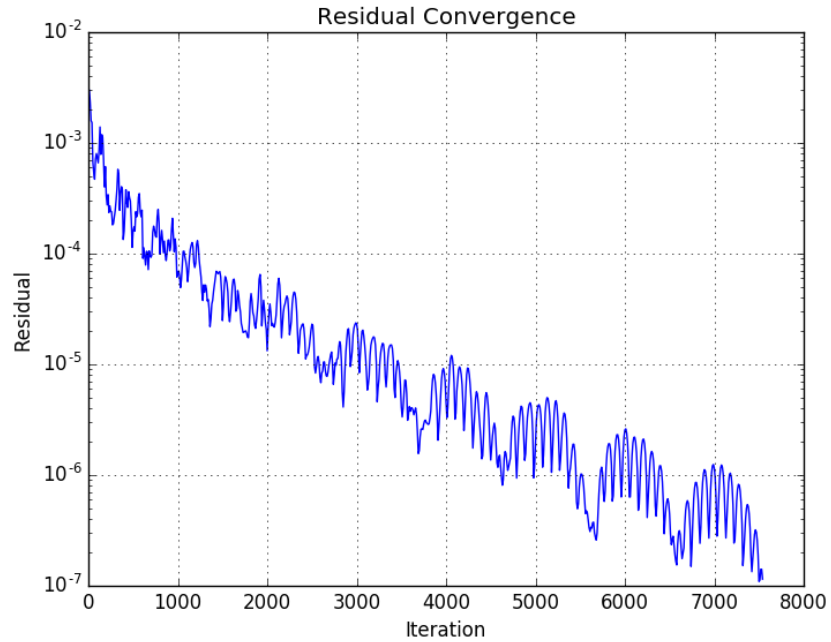


Pressure coefficient for mesh 0, second-order method

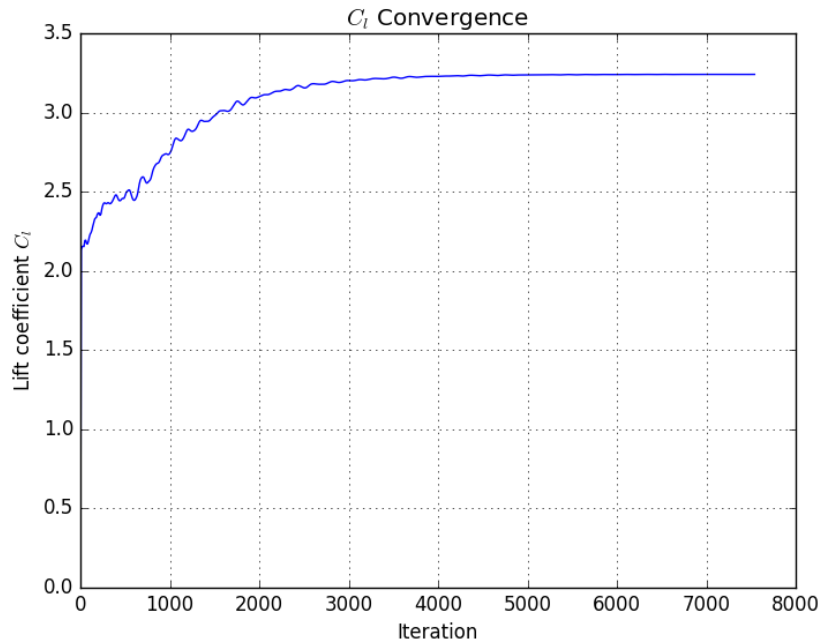


Streamline contour for mesh 0, second-order method

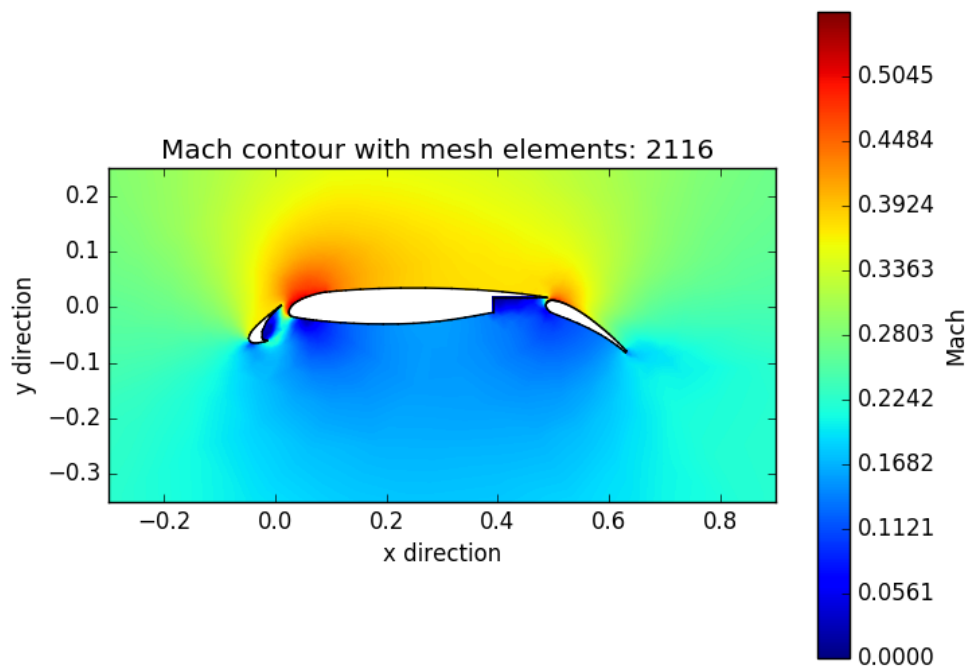
Mesh 1



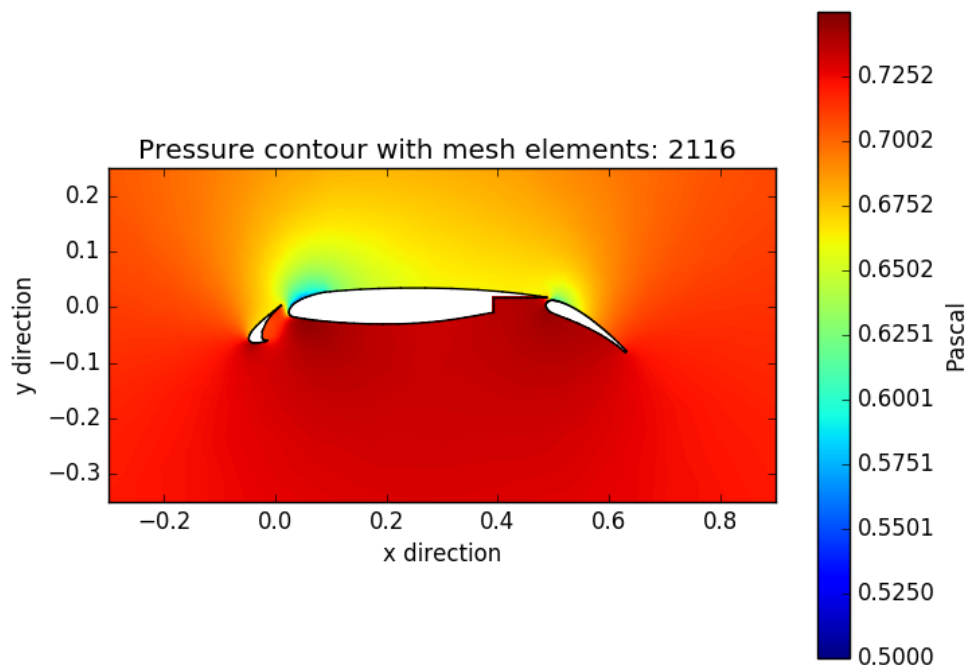
Residual for mesh 1, second-order method



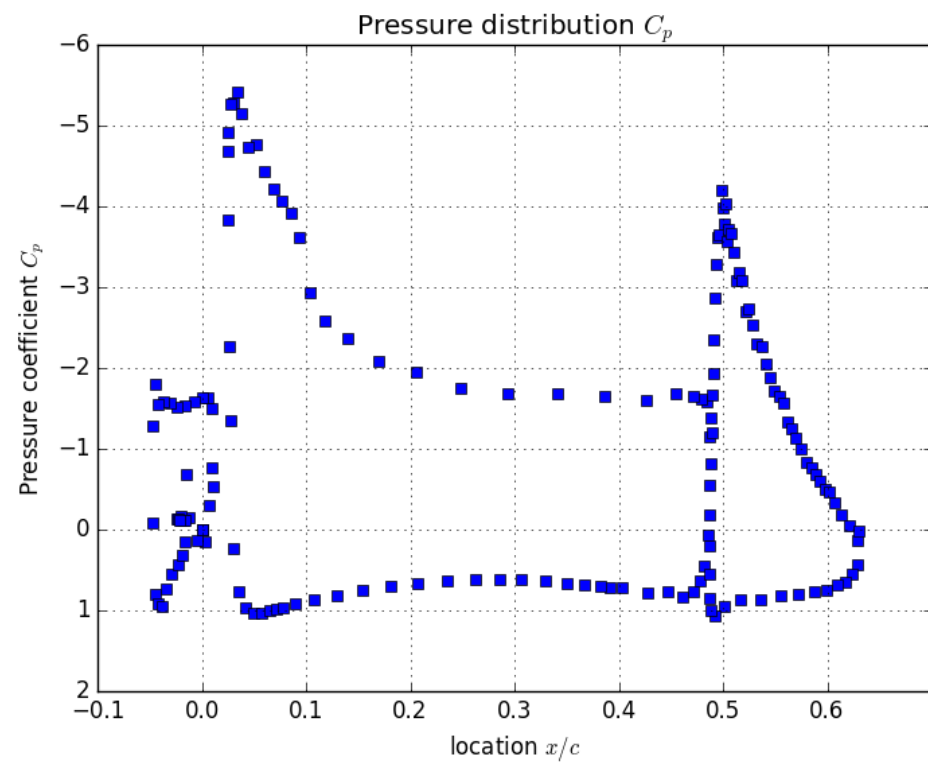
Lift coefficient for mesh 1, second-order method



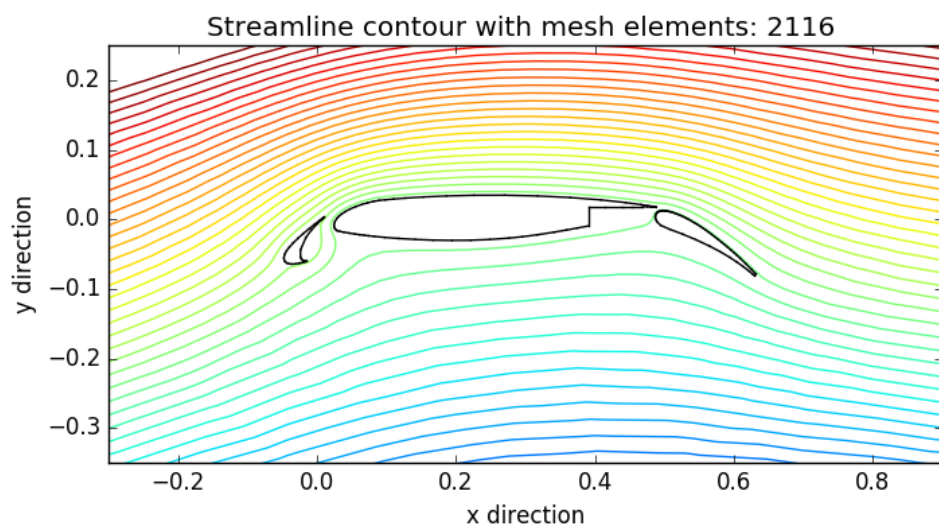
Mach contour for mesh 1, second-order method



Pressure contour for mesh 1, second-order method

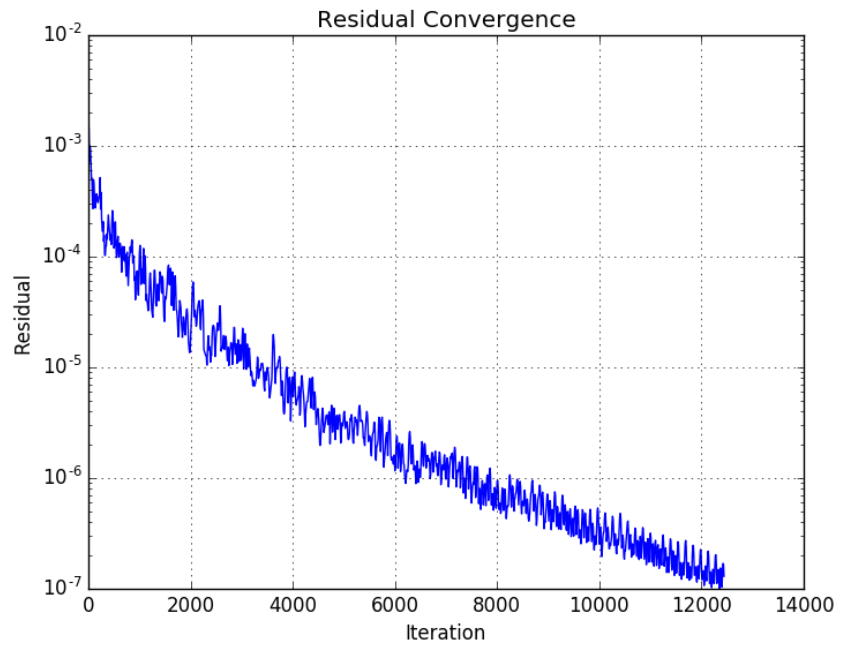


Pressure coefficient for mesh 1, second-order method

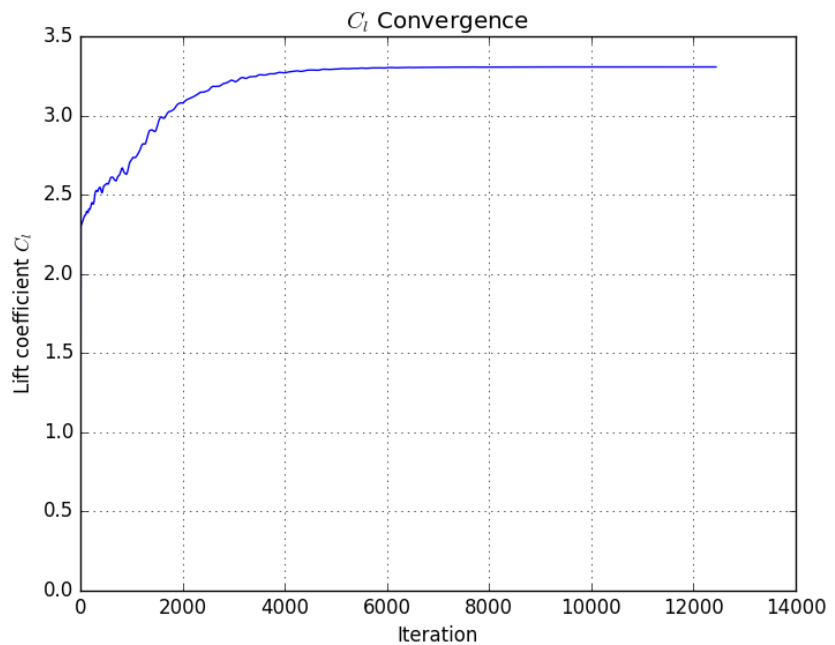


Streamline contour for mesh 1, second-order method

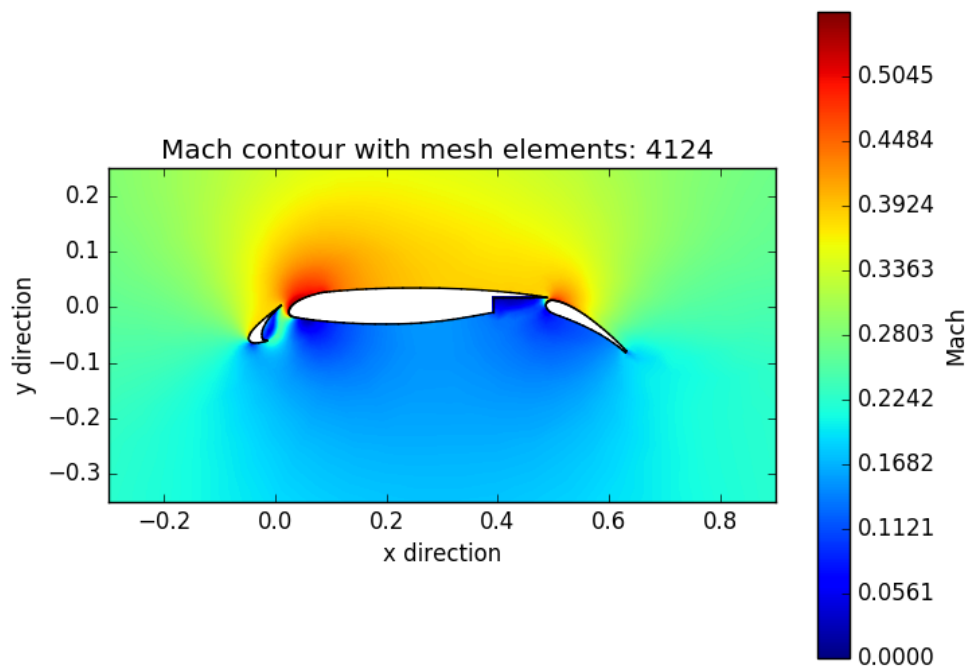
Mesh 2



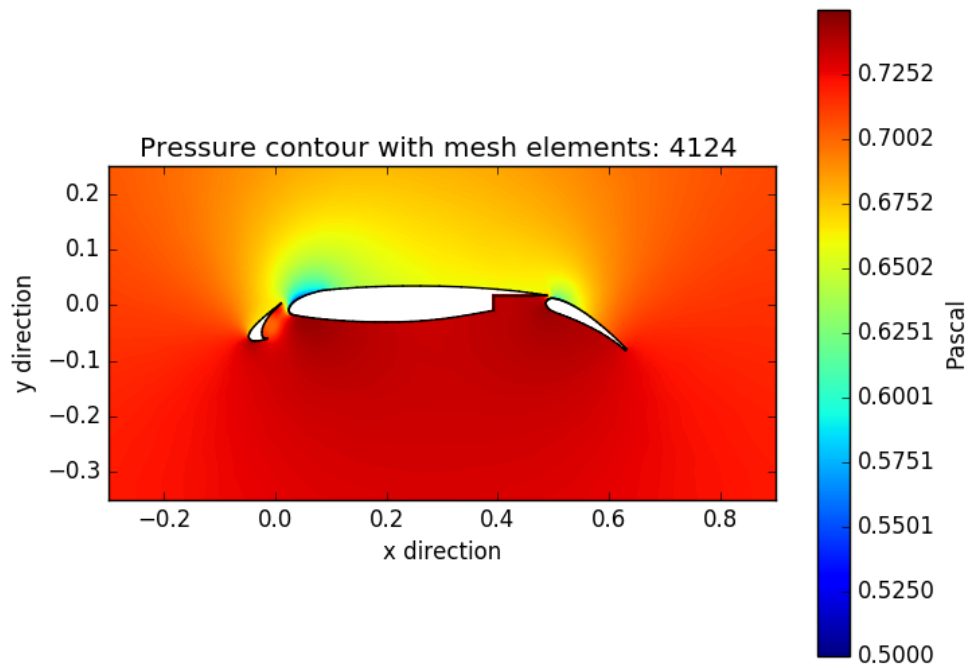
Residual for mesh 2, second-order method



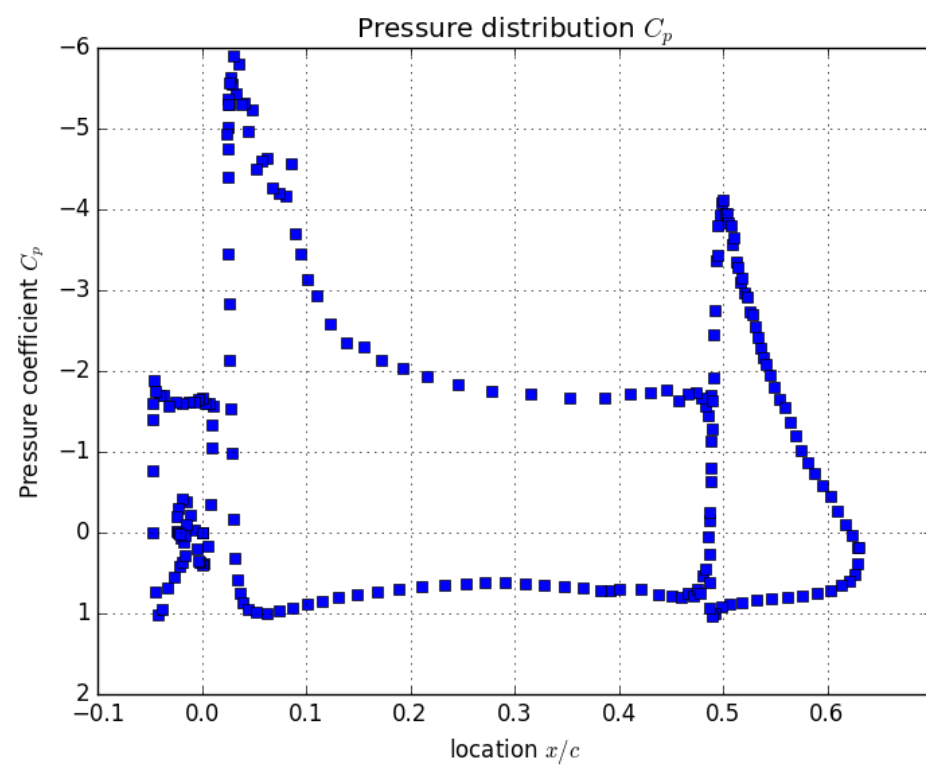
Lift coefficient for mesh 2, second-order method



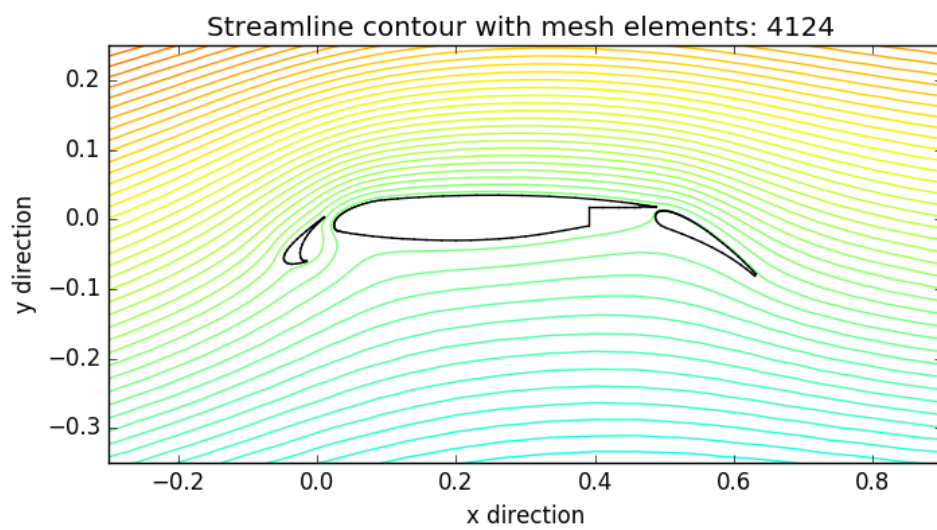
Mach contour for mesh 2, second-order method



Pressure contour for mesh 2, second-order method

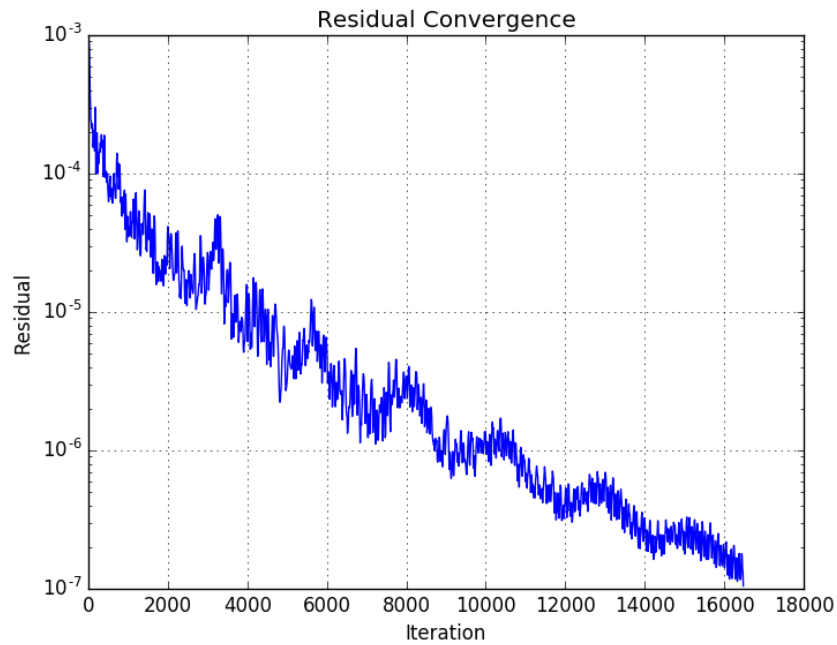


Pressure coefficient for mesh 2, second-order method

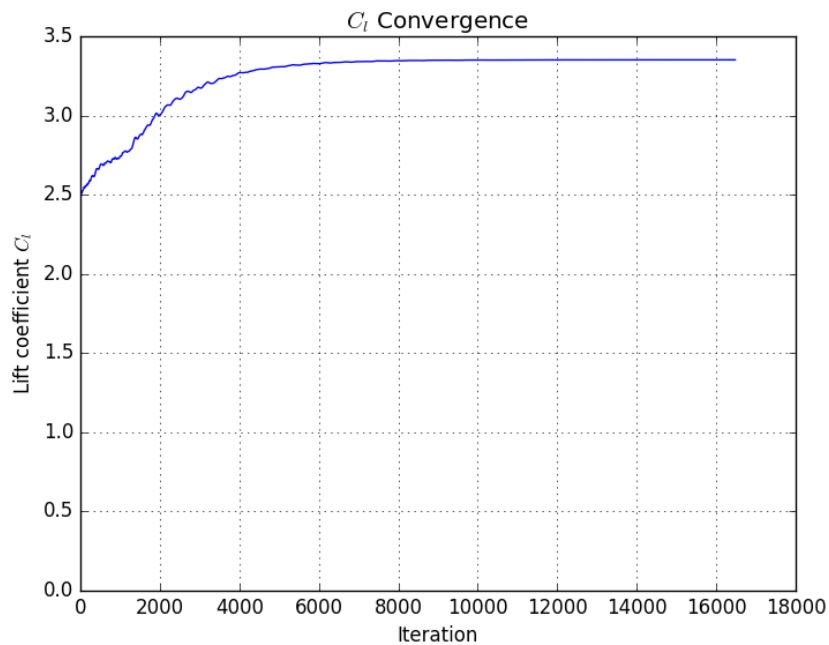


Streamline contour for mesh 2, second-order method

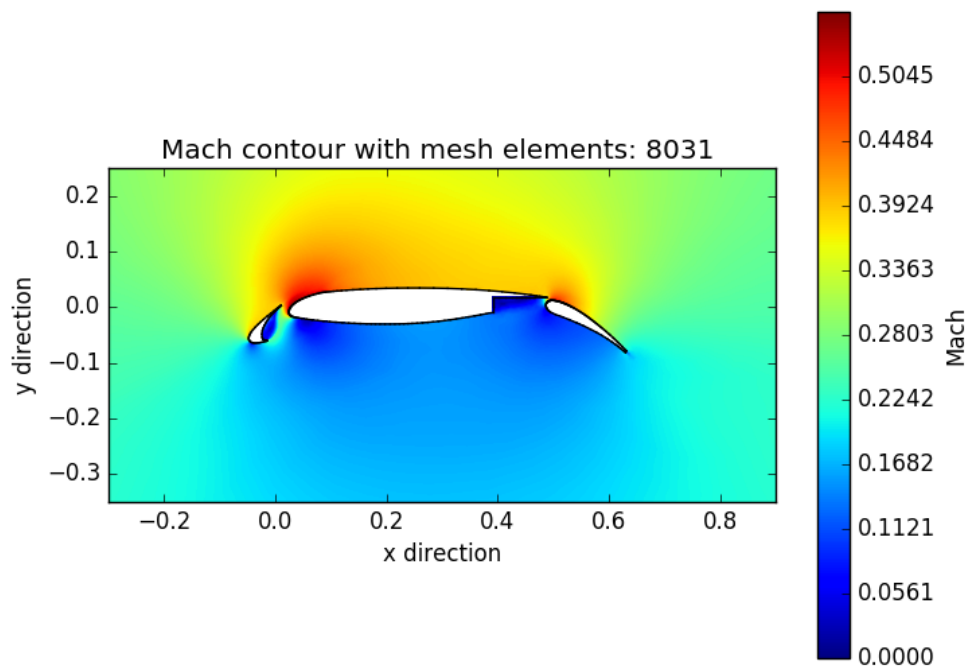
Mesh 3



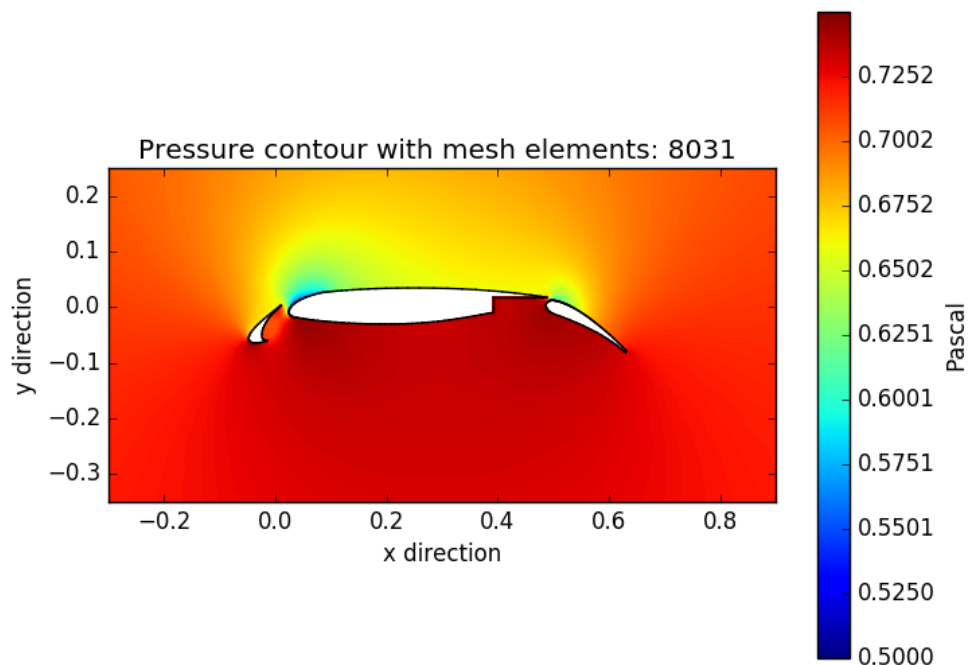
Residual for mesh 3, second-order method



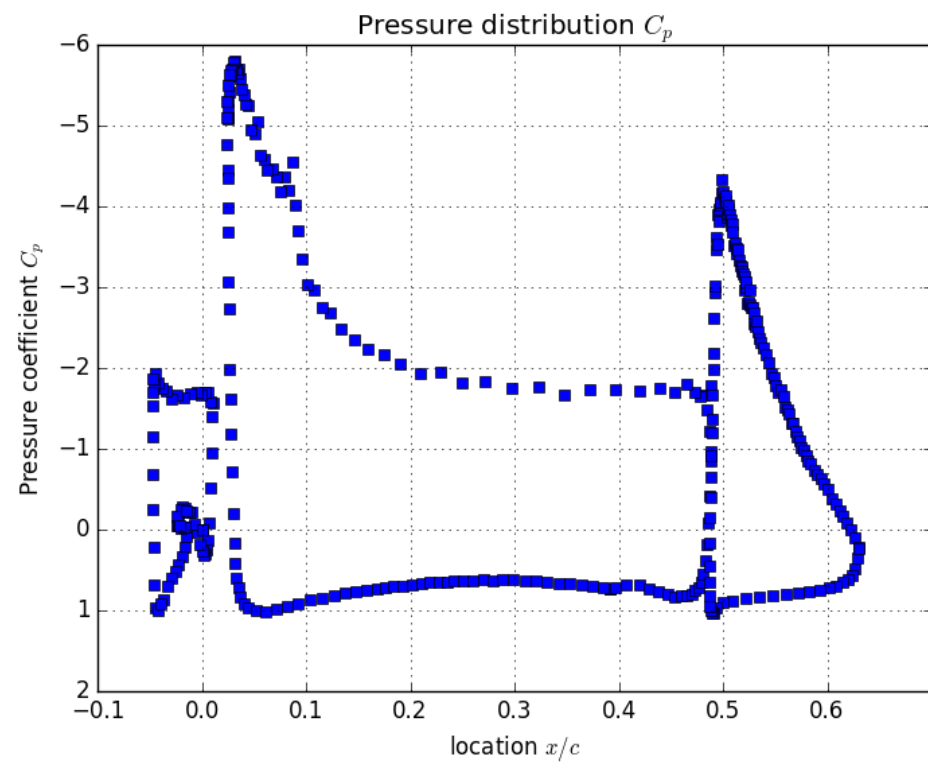
Lift coefficient for mesh 3, second-order method



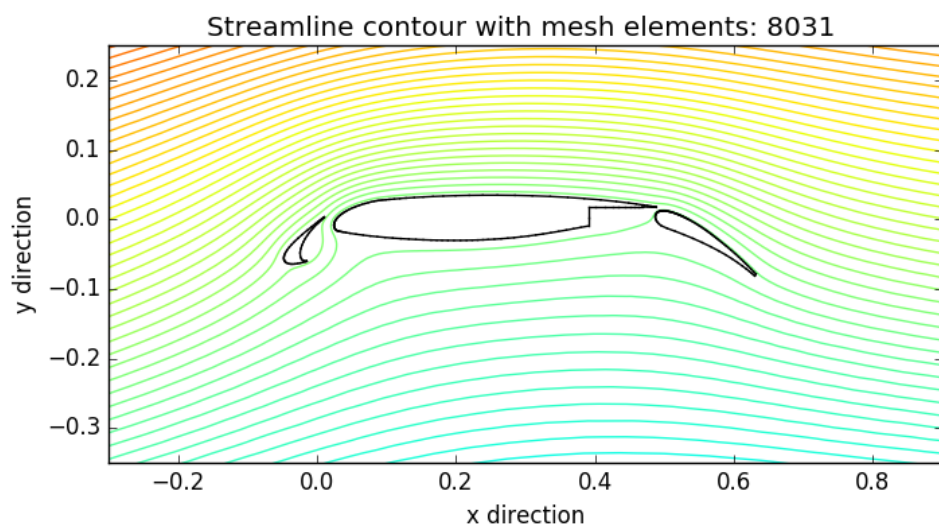
Mach contour for mesh 3, second-order method



Pressure contour for mesh 3, second-order method



Pressure coefficient for mesh 3, second-order method



Streamline contour for mesh 3, second-order method